CHEMISTRY
A EUROPEAN JOURNAL

DOI: 10.1002/chem.200600447

Three-Dimensional Six-Connecting Organic Building Blocks Based on Polychlorotriphenylmethyl Units—Synthesis, Self-Assembly, and Magnetic Properties

Nans Roques,[a] Daniel Maspoch,[a] Klaus Wurst,[b] Daniel Ruiz-Molina,[a] Concepció Rovira,[a] and Jaume Veciana*[a]

Abstract: The synthesis of a three-dimensional, six-connecting, organic building block based on a robust, rigid, and open-shell polychlorotriphenylmethyl (PTM) unit (radical **1**) is reported, and its self-assembly properties are described in detail. The tendencies of this highly polar molecule and its hydrogenated precursor, compound **4**, to form hydrogen bonds with oxygenated solvents ([**1**·THF_6] and [**4**·THF_6]) were reduced by replacing THF with diethyl ether in the crystallization process to yield two-dimensional (2D) hydrogen-bonded structures ([**1**·$(Et_2O)_3$] and [**4**·$(Et_2O)_3$]). The presence of direct hydrogen bonds between the radicals in the latter phase of **1** gives rise to very weak ferromagnetic intermolecular interactions at low temperatures, whereas when the radicals are isolated by THF molecules these interactions are antiferromagnetic and very weak. The role played by the carboxylic groups not only in the self-assembly properties but also in the transmission of the magnetic interactions has been illustrated by determination of the crystal structure and measurement of the magnetic properties of the corresponding hexaester radical **6**, in which the close packing of molecular units gives rise to weak antiferromagnetic intermolecular interactions. Attempts to avoid solvation of the molecules in the solid state and to increase the structural and magnetic dimensionality were pursued by recrystallization of both compounds **1** and **4** from concentrated nitric acid, affording two three-dimensional (3D) robust hydrogen-bonded structures. While the structure obtained with compound **4** is characterized by the presence of polar channels and boxes containing water guest molecules along the *c* axis, radical **1** was oxidized to the corresponding fuchsone **10**, which presented a completely different close-packed, guest-free structure.

Keywords: free radicals · hexacarboxylic acids · magnetic properties · self-assembly · structure dimensionality

Introduction

Control of molecular organization is an essential aspect of the development of purely organic solids with remarkable physical or chemical properties and structural characteristics.[1] Whereas supramolecular chemistry has allowed access to numerous examples of molecular organizations in one and two dimensions,[2,3] those organized in three dimensions are still challenging propositions.[4] The fairly limited number of purely organic three-dimensional assemblies reported so far may be explained by the difficulties involved in synthesizing well-programmed molecular building blocks,[5] with regard to the positions of the noncovalent interactive sites, molecular shape, rigidity, and amphiphilicity,[6,7] and also by the complexity inherent in obtaining the required fine sophisticated self-assemblies through noncovalent interactions.[8]

[a] Dr. N. Roques, Dr. D. Maspoch, Dr. D. Ruiz-Molina, Prof. C. Rovira, Prof. J. Veciana
Institut de Ciènca de Materials de Barcelona (CSIC)
Campus Universitari, 08193 Bellaterra, Barcelona, Catalonia (Spain)
Fax: (+34) 93-580-5729
E-mail: vecianaj@icmab.es

[b] Dr. K. Wurst
Institut für Allgemeine Anorganische und Theoretische Chemie
Universitat Innsbruck, 6020, Innrain 52a
Innsbruck (Austria)

Supporting information for this article is available on the WWW under http://www.chemeurj.org/ or from the author. It includes two figures illustrating the supramolecular motifs involved in the self-assembly of molecule **10**.

Such synthetic and structural considerations are even more difficult to fulfill in the case of purely organic magnetic materials based on the self-assembly of open-shell tectons.[1d,9] Different families of open-shell tectons have been used with this as a goal and it has, for instance, been shown that the relatively small size and flatness of verdazyl radicals enables them to π-stack, resulting in very strong magnetic exchange interactions despite the radical centers being quite far apart.[10] Other examples include the series of dithiadiazolyl and dithiazolyl radicals, which exhibit bulk magnetic order and room temperature bistability.[11] Nevertheless, the family of open-shell tectons most widely used up to now is that of α-nitronyl nitroxide, α-imino nitroxide, or *tert*-butyl nitroxide derivatives, because of their high stabilities and the abilities of their nitroxide groups to act as hydrogen-bond acceptors, so the self-assembly of such nitroxide-based building blocks substituted with one or several hydrogen-bond donors, such as phenol,[12] boronic acid,[13] imidazole,[14] benzimidazole,[15] triazole,[16] uracil,[17] pyrazole,[18] phenylacetylene,[19] or benzoic acid[20], has been extensively studied. The resulting synthons enable both structural control and transmission of magnetic interactions between the radical molecules through strong (O−H···O) or weak (CH_3···O) hydrogen bonds.[12,21] This approach shows that the structural dimensionality of the material—and hence the propagation of the magnetic interactions through the supramolecular structure—may to some extent be controlled through the design of radical molecules bearing hydrogen-bond donor and acceptor groups. However, the difficulties lie in determining the exact strength and the nature of the magnetic interactions through the supramolecular pathways, as additional undesired intermolecular through-space interactions are often present in the solid state and very frequently obstruct proper design of magnetic exchange pathways.[12e,17,18]

To circumvent such inconveniences, our group has initiated a strategy based on the synthesis and study of polychlorotriphenylmethyl (PTM) radicals functionalized with carboxylic groups. Our interest in these radicals is threefold. Firstly, they exhibit high thermal and chemical stability. Secondly, from a structural point of view, the rigidity and bulkiness of this family of open-shell molecules[22] would be expected to prevent close packing to form robust networks[23] and to minimize undesired through-space magnetic interactions in the solid state. Last but not least, among the numerous functional groups that have been used to build self-assembled networks, the choice of carboxylic acid groups is dictated by the wide range of supramolecular synthons potentially offered by their presence,[24] their well known capacity to form strong and directional hydrogen bonds, and also their ability to promote magnetic interactions between radical species.[20] We have thus previously described the synthesis, self-assembly, and magnetic properties of two PTM radicals substituted with two (PTMDC) and three (PTMTC) carboxylic acid functions in *para* positions by this approach. Consistently with their rigidity and their structural analogy with the isophthalic and trimesic acids, the self-assembly of these two radicals created noninterpenetrated open-framework structures consisting of 2D hydrogen-bonded layers.[23] Indeed, while an example of a purely organic open-framework (POROF-1) with dominant antiferromagnetic interactions was obtained with the diacid radical,[25] the self-assembly of the triacid radical produced a robust, porous, extended network (POROF-2), giving rise to highly polar nanotubular channels for the first time, together with ferromagnetic ordering at low temperatures.[26]

As a natural evolution due to the interest engendered by the previously described work, we report here the synthesis, supramolecular organization, and magnetic properties of radical **1**, which is substituted with six carboxylic acid groups at the *meta* positions of the phenyl rings. In addition to the synthetic challenge implied in its synthesis and characterization,[27,28] the changes both in the number (six) and in the location (*meta* positions) of the carboxylic groups around the PTM moiety would be expected to afford new 3D assemblies, as recently demonstrated in the case of triphenylmethane-based polyphenols.[29] Moreover, the presence of six carboxylic groups in radical **1** might be expected to enhance the number of magnetic exchange pathways between PTM radicals by means of the hydrogen-bonding network.[30]

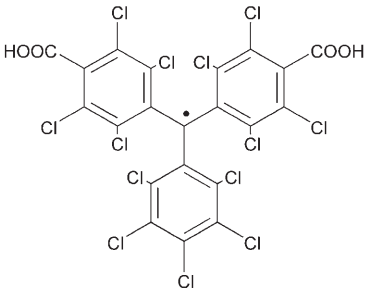

PTMDC

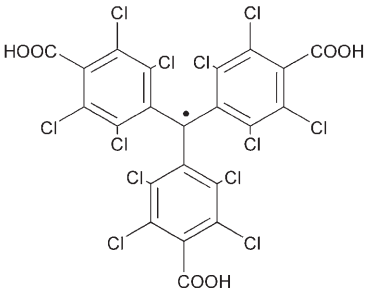

PTMTC

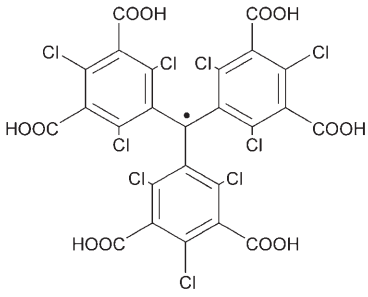

PTMHC, **1**

Results and Discussion

Synthesis: Radical **1** was prepared by the original six-step procedure detailed in Scheme 1. A Friedel–Crafts reaction performed with aluminum trichloride as a catalyst and with a large excess of 1,3,5-trichlorobenzene over chloroform (9:1) enabled the formation of compound **2**, possessing a PTM skeleton with six hydrogen atoms, all in *meta* positions. Dichloromethyl groups were then introduced at the *meta* positions by treatment of **2** with an excess of chloroform in the presence of aluminum trichloride to afford compound **3** as a white solid.[31] Subsequently, the dichloromethyl groups were converted to provide the corresponding hexacarboxylic acid **4** through hydrolysis/oxidation by treatment of **3** with 20% oleum.[25,26] To the best of our knowledge, this is the first time that conditions of this kind have been used to provide access to a hexacarboxylic acid molecule. The next step was the formation of the radical species by the methodology previously used to prepare the *para*-di- and -tricarboxylic acid radicals PTMDC and PTMTC. This one-pot reaction consists of two steps, starting with the formation of the corresponding polyanion and continuing with the oxidation of the central carbanion. Surprisingly, this reaction did not work for the hexacarboxylic species. Indeed, whilst in the cases of the di- and triacid PTM compounds the formation of the anionic species had been complete within three days, treatment of the hexa-acid **4** under the same conditions only afforded the corresponding hexa-anion through deprotonation of the acidic groups, as confirmed by UV/visible measurements. Increasing of the reaction time and/or modification of the reaction conditions (change of base, solvent, or reaction temperature) either gave the same result or, when reaction times were longer than one month, resulted in the transformation of the hexacarboxylate derivative into unknown compounds. It seems reasonable to think that the negative shell produced by the presence of the six carboxylate groups located in *meta* positions impedes easy removal of the hydrogen atom located in the central carbon atom of the PTM unit.

To overcome these difficulties, compound **4** was first converted into the hexaester **5** with diazomethane.[32] Afterwards, treatment of **5** with tetrabutylammonium hydroxide yielded the intermediate carbanion, which presented the absorption band characteristic of an anionic PTM species at 520 nm.[33] This intermediate was then oxidized to the corresponding radical **6** by addition of an excess of *para*-chloranil.

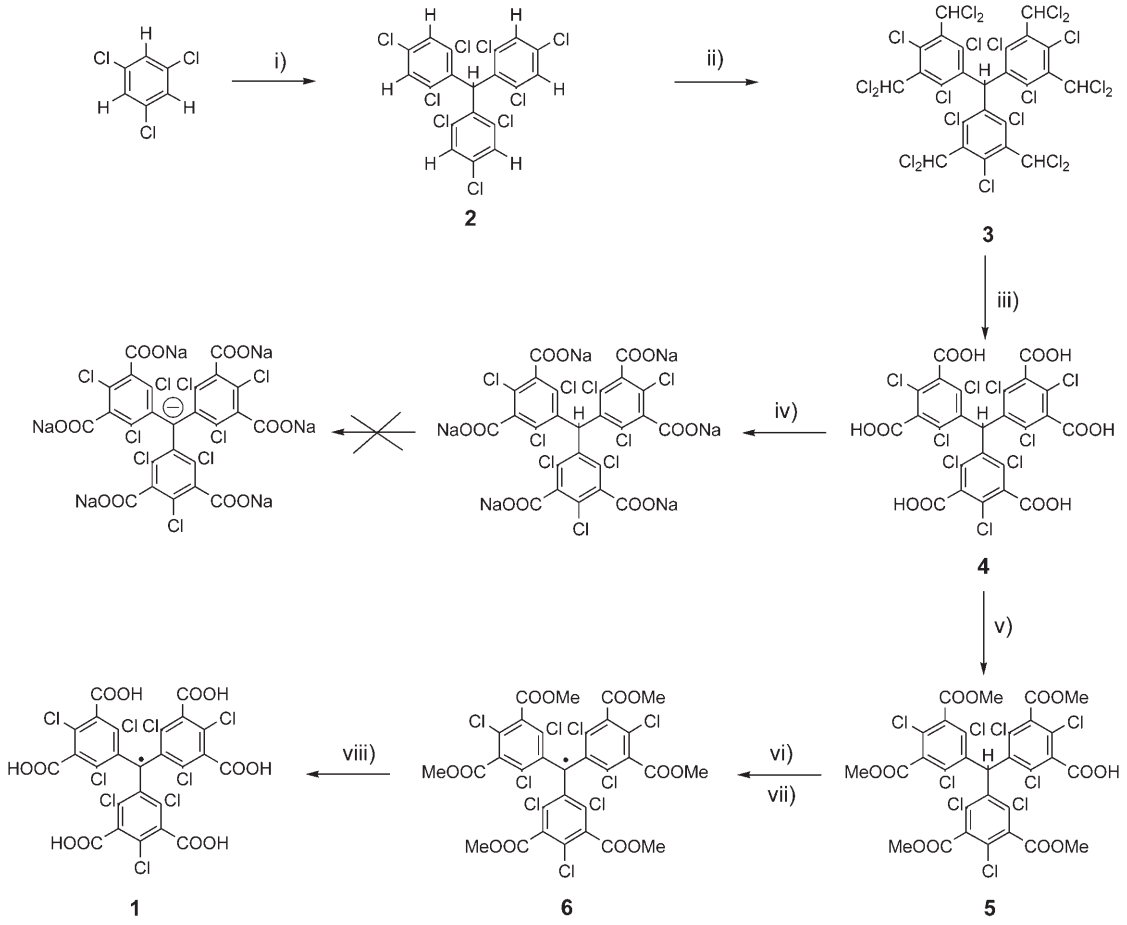

Scheme 1. i) $AlCl_3$, $CHCl_3$, excess of 1,3,5-trichlorobenzene, 110 °C (yield: 70%); ii) $AlCl_3$, excess of $CHCl_3$, 90 °C (70%). iii) Oleum (20%), 150 °C (75%); iv) Excess of NaOH, DMSO, RT; v) diazomethane, Et_2O, 25 °C (80%); vi) *n*-Bu_4NOH, THF, 25 °C, vii) *p*-Chloranil, THF, 25 °C (80%); viii) H_2SO_4, 100 °C (90%).

The methyl ester groups were finally removed by heating compound **6** in concentrated sulfuric acid to afford radical **1** in an overall yield of 21% after the six steps. Remarkable is the solubility of molecules **1** and **4** in solvents, such as water, ethers, and alcohols.

Molecular and crystalline structures of 1 and 4: Several attempts to recrystallize radical **1** and its hydrogenated precursor **4** were made with various solvent mixtures, concentrations, and crystallization techniques. Most of these failed, giving amorphous solids when mixtures involving nonoxygenated solvents, such as chloroform or dichloromethane, were used to dissolve the hexa-acid derivatives. In contrast, two different crystalline solvate phases were obtained by slow diffusion of *n*-hexane over either THF or Et_2O solutions in the cases both of compound **1** and of compound **4**. It is important to emphasize that in spite of the change in the hybridization state of the central methyl carbon atom between radical **1** and its hydrogenated precursor **4**, associated with the transformation from a planar to a tetrahedral configuration, the resulting crystallographic phases of the two compounds are very similar. Crystallographic data for the different crystalline phases obtained are shown in Table 1.

THF solvates: Crystals of **4** were obtained by layering a THF solution of the hexa-acid derivative with *n*-hexane. Although the crystals were found to lose crystallinity once they had been removed from the mother liquor, the X-ray structure was determined by handling the crystals with care at low temperatures. A representative ORTEP drawing for the PTM unit is shown in Figure 1. This solvate crystallizes in the *R*-3 trigonal space group, with six molecules of hexa-acid **4** and 36 molecules of THF in the unit cell.

The molecule possesses a threefold rotation axis that passes through the central carbon atom (C3). As a conse-

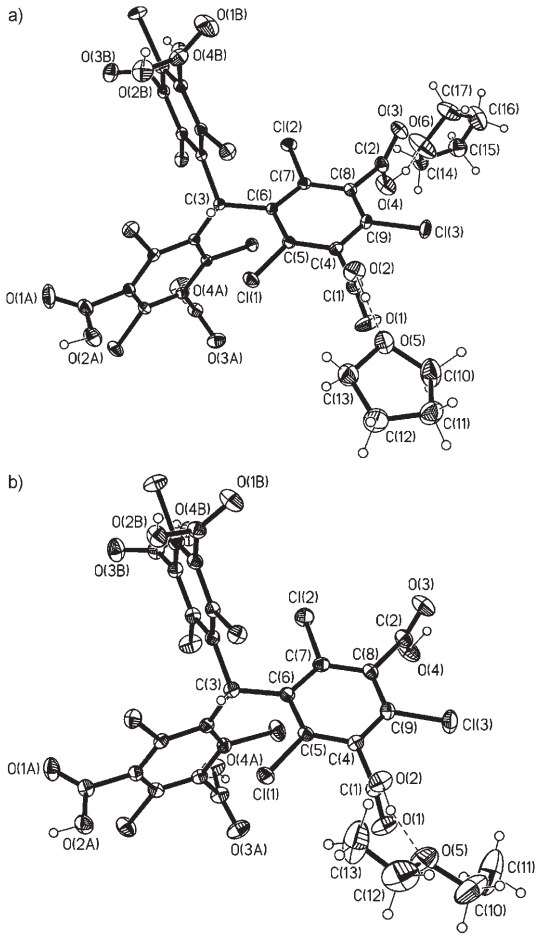

Figure 1. Representative ORTEP views of the molecule common to [**4**·THF_6] (a) and [**4**·$(Et_2O)_3$] (b). Thermal ellipsoids are set at 20% probability and symmetry-related solvent molecules have been omitted for clarity (representative atoms labeled).

Table 1. Crystallographic data and structure refinement of solvates of **1** and **4** and of compounds **6** and **10**.

	[**4**·THF_6]	[**4**·$(Et_2O)_3$]	[**4**·$(H_2O)_{1.5}$]	**6**	[**1**·THF_6]	[**1**·$(Et_2O)_3$]	**10**
formula	$C_{49}H_{55}Cl_9O_{18}$	$C_{37}H_{37}Cl_9O_{15}$	$C_{25}H_{10}Cl_9O_{13.5}$	$C_{31}H_{18}Cl_9O_{12}$	$C_{49}H_{54}Cl_9O_{18}$	$C_{37}H_{36}Cl_9O_{15}$	$C_{25}H_6Cl_8O_{13}$
M_r	1250.98	1040.72	845.38	901.50	1249.97	1039.71	797.90
lattice type	trigonal	trigonal	tetragonal	monoclinic	trigonal	trigonal	orthorhombic
space group	*R*-3	*R*-3	$P\text{-}42_1c$	*C*2/c	*R*-3	*R*-3	Ccca
a [Å]	24.8944(6)	15.6119(5)	20.7352(3)	23.0403(4)	24.9133(6)	15.6488(8)	14.3641(3)
b [Å]	24.8944(5)	15.6119(5)	20.7352(4)	13.6539(5)	24.9133(8)	15.6448(6)	21.6196(3)
c [Å]	15.3111(3)	33.7497(5)	15.2669(5)	12.7045(6)	15.0874(8)	33.8402(7)	19.5798(5)
α [°]	90	90	90	90	90	90	90
β [°]	90	90	90	105.588(2)	90	90	90
γ [°]	120	120	90	90	120	120	90
V [Å^3]	8217.5(3)	7123.8(3)	6564.0(3)	3849.7(2)	8109.7(5)	7176.7(5)	6080.4(2)
Z	6	6	8	4	6	6	8
ρ_{calcd} [g cm^{-3}]	1.517	1.456	1.711	1.555	1.536	1.443	1.743
T [K]	213(2)	233(2)	233(2)	233(2)	233(2)	233(2)	233(2)
unique reflections	3207	2069	4563	3377	2347	2211	2391
reflections observed [$I>2\sigma(I)$]	2842	1777	4150	2730	1761	1880	2009
*R*1 (all data)	0.0517	0.0543	0.0535	0.0517	0.0903	0.0679	0.0578
*R*1 [$I>2\sigma(I)$]	0.0451	0.0464	0.0472	0.0377	0.0678	0.0588	0.0478
*wR*2 (all data)	0.1133	0.1301	0.1203	0.0978	0.2055	0.1703	0.1408
*wR*2 [$I>2\sigma(I)$]	0.1096	0.1232	0.1167	0.0920	0.1884	0.1624	0.1326

quence, the dihedral angles between the mean planes of the three polychlorinated aromatic rings and that of the three bridgehead carbon atoms (the reference plane) are equal to 58°, causing the molecule to adopt a three-bladed, propellerlike conformation with a given *P* (plus) or *M* (minus) helicity, as is usual for these compounds.[34] Because of the steric hindrance from the chlorine atoms in the positions *ortho* to each carboxylate group, the carboxylates are twisted by 80 (C9-C4-C1-O1) and 88° (C9-C8-C2-O3) with respect to the ring to which they are bonded, with the two acidic hydrogen atoms lying above and below the plane of the phenyl ring.

Each carboxylic acid group forms one strong hydrogen bond with a THF molecule, with bond lengths of 1.75(2) and 1.79(4) Å (O2−H···O5 and O4−H···O6) and bond angles of 167(5) and 147(6)° (O2−H···O5 and O4−H···O6), respectively (Figure 2a–b), so [**4**·THF_6] units are formed in the crystal. Their self-assembly is assumed to take place through the formation of weak C=O···HC(THF) hydrogen bonds (18 bonds in [**4**·THF_6] units) with bond lengths of 2.67, 2.70, and 2.72 Å (C12−H···O3, C15−H···O2, C14−H···O4) and bond angles of 139, 135, and 159° (C12−H···O4, C15−H···O2, C14−H···O4). The resulting supramolecular columns are made up of molecules of **4** with alternating *P* and *M* helicities in their three-bladed, propellerlike conformations (Figure 2c–d), the alternating distances between C3 atoms of different molecules being 6.86 and 8.45 Å. Additional weak hydrogen bonds between THF molecules of [**4**·THF_6] units belonging to different columns (six by unit: C16−H···O5 = 2.7 Å; C15−H···O5 = 129°) enable their close packing, resulting in a honeycomblike arrangement of the THF molecules around the molecules of hexa-acid when the structure is viewed along the *c* axis (Figure 2e).

Slow diffusion of *n*-hexane into a THF solution of radical **1** allowed small crystals, suitable for single-crystal X-ray analysis, of the radical solvate [**1**·THF_6] to be obtained. This radical solvate also crystallizes in the *R*-3 trigonal space group with six molecules of **1** and 36 molecules of THF in the unit cell. The change in the hybridization of the central carbon atom (sp^2 in **1** versus sp^3 in **4**) is translated into a decrease in the value of the angles between the phenyl rings and the reference plane of the molecule (55° versus 58°), in which the central carbon (C3) atom and the three aromatic bridgehead carbon atoms (C6) are now fixed. This change in the central carbon atom hybridization state is also accompanied by a shortening of the C3−$C_{bridgehead}$ bond length, 1.478(5) Å in **1** versus 1.548(3) Å in **4**, and an increase in the C−C3−C angles from 114.8(2) in **4** to 119.96(3) in **1**. As in [**4**·THF_6] solvate, the three equivalent phenyl rings adopt a propellerlike arrangement around the central carbon atom, the carboxylic acid groups making angles of 87° with them (C9-C4-C1-O1 ≈ C9-C8-C2-O3), with acid hydrogen atoms lying above and below the phenyl ring to which they are attached. The carboxylic hydrogen atoms are involved in hydrogen bonds with highly disordered THF molecules. Hydrogen atoms of the THF molecules were not found and not calculated, but the analogy between **1** and **4** enables us to predict quite similar supramolecular arrangements of the two solvates. However, small structural changes in **1** have given rise to alternating intermolecular C3–C3 distances of 7.51 and 7.57 Å and to slight changes in the cell parameters.

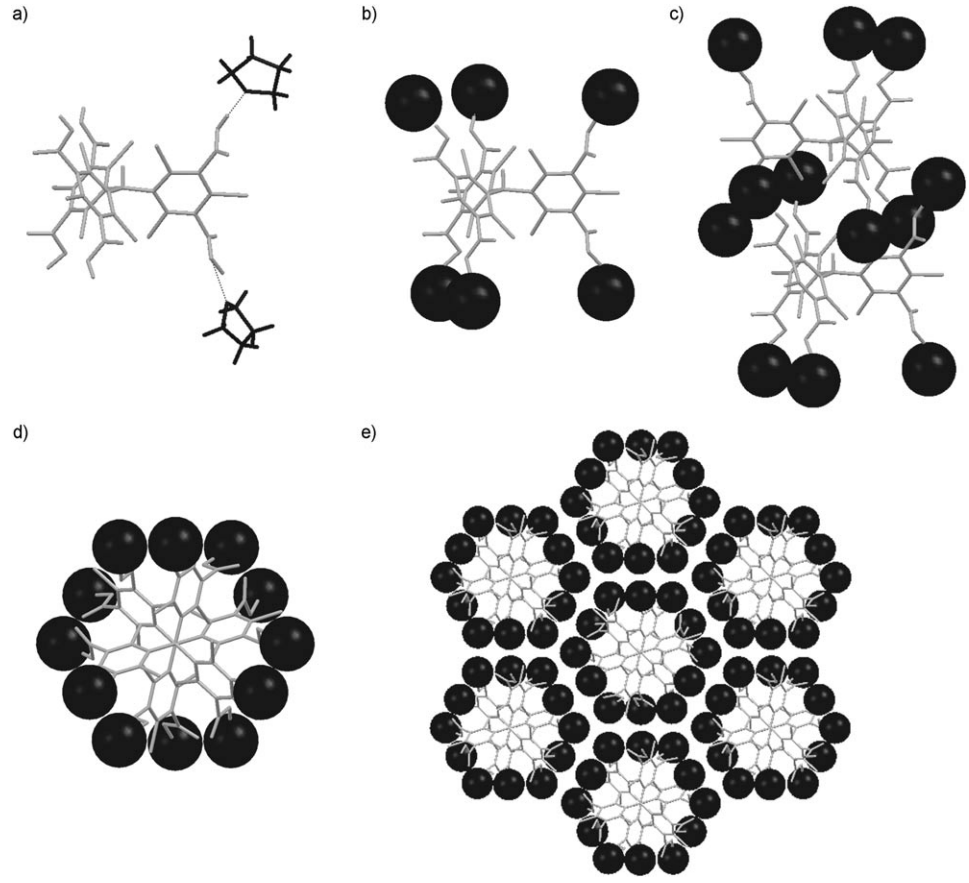

Figure 2. Crystal structure of [**4**·THF_6]. a) Hydrogen bonds (dashed lines) with THF molecules. b) View of the supramolecular [**4**·THF_6] cluster (THF molecules are represented as spheres for clarity). c) Packing of the clusters along the *c* axis and d) top view of the resulting column. e) Self-assembly of the columns yield a honeycomblike arrangement of the THF molecules around the molecules of **4**.

Diethyl ether solvates: Crystals of a different solvate of **4** were grown by diffusing *n*-hexane into an Et_2O solution of **4**. As

in the case of THF solvates, the crystals were unstable when they were removed from the mother liquor, but the solvate's X-ray structure could be determined by handling the crystals with care at low temperatures. This new solvate, [**4**·(Et_2O)$_3$], crystallizes in the *R*-3 trigonal space group with six molecules of hexa-acid and eighteen molecules of Et_2O in the unit cell. The molecule possesses a threefold rotation axis that passes through the central carbon atom (C3), and the phenyl rings are twisted by angles of 55° with respect to the reference plane of the molecule. Because of the presence of the chlorine atoms at the *ortho* positions, the angles between the carboxylic acid groups and the phenyl rings to which they are bonded have values of 84 (C9-C4-C1-O1) and 83° (C9-C8-C2-O3). In this conformation, the acidic hydrogen atoms of each of the carboxylic groups lie above and below the mean plane of the phenyl ring to which they are bonded.

The most striking difference with the THF solvate is the presence of several direct hydrogen bonds between molecules of hexa-acid, resulting in the formation of 2D hydrogen-bonded corrugated layers running in the *ab* plane. The main repetitive unit consists of an $R_6^6(48)$ hydrogen-bonded hexamer formed by molecules of hexa-acid with alternation of their *P* and *M* helicities in their three-bladed, propeller-like conformations (Figure 3a–c). In this hexamer, each molecule of hexa-acid is hydrogen-bonded with two neighboring hexa-acid units through one carboxylic group, with a bond length of 1.78(3) Å (O4−H···O1) and a bond angle of 167(6)° (O4−H···O1). The remaining carboxylic group located in the same phenyl ring is involved in the formation of one hydrogen bond with an Et_2O molecule, with a bond length of 1.72(3) Å (O2−H···O5) and a bond angle of 167(6)° (O2−H···O5). This carboxylic acid–Et_2O interaction is reinforced by a supplementary weak hydrogen bond between the carbonyl group and one of the methyl groups of the solvent molecule (O1···H−C11 = 2.62 Å and O1···H−C11 = 135°).[35] The same kind of weak hydrogen bond is also found between this Et_2O molecule and a molecule of hexa-acid presenting the same helicity in the layer (C11−H···O2 = 2.6 Å and C11−H···O2 = 165°).

As every molecule has six carboxylic acid groups—half of them involved in hydrogen bonds with neighboring molecules of hexa-acid and half with solvent molecules—each molecule of **4** participates in the formation of three identical hexameric units, resulting in polar windows that propagate along the *ab* plane (Figure 3d). Three Et_2O molecules are localized on both sides of each polar window and contribute to isolating one layer from each other, avoiding the formation of hydrogen bonds or Cl···Cl and/or Cl···O short contacts between molecules of hexa-acid. Interdigitation of sol-

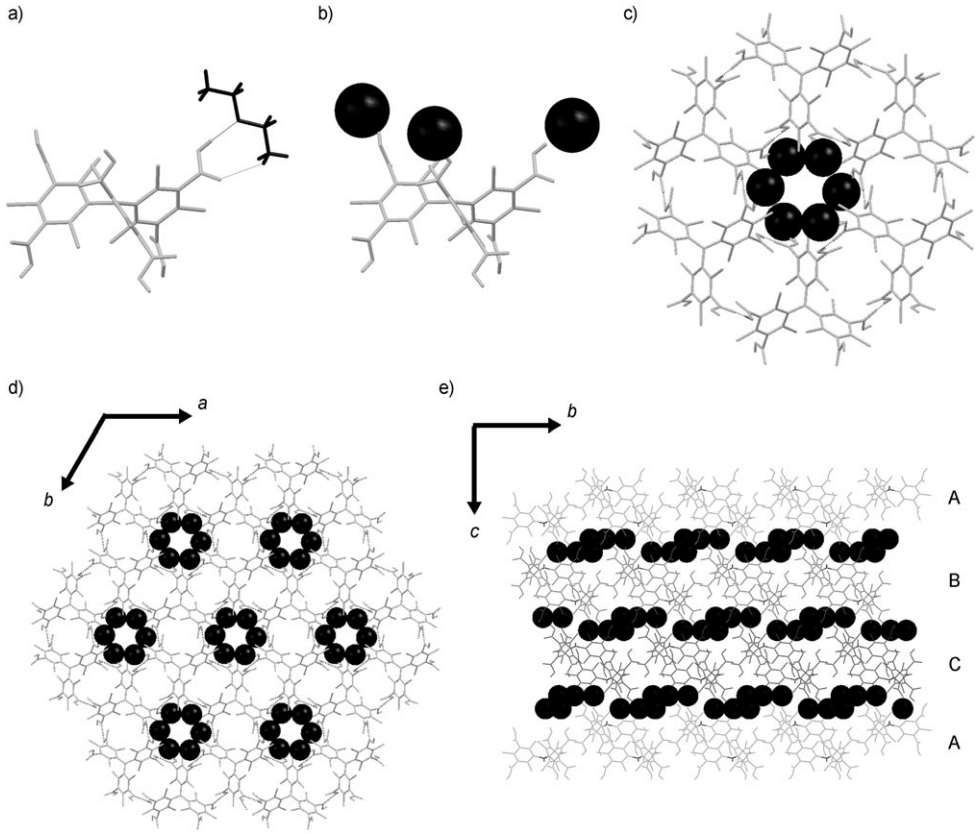

Figure 3. Crystal structure of [**4**·(Et_2O)$_3$]. a) Hydrogen bonds (dashed lines) with diethyl ether molecule. b) View of the supramolecular [**4**·(Et_2O)$_3$] unit (Et_2O molecules are represented as spheres for clarity). c) $R_6^6(48)$ hexamer and d) extended hydrogen-bonded corrugated layer (clear spheres represent ether molecules below the layer). e) ABC arrangement of the layers, isolated from one another by solvent molecules.

vent molecules belonging to neighboring layers yields an ABC packing of the layers along the *c* axis (Figure 3e). This packing is achieved through two types of weak hydrogen bonds involving carboxylic groups of the PTM units and CH_2 or CH_3 groups of the Et_2O molecules (O1···H−C10 and O3···H−C13 with bond lengths of 2.66 and 2.72 Å and bond angles of 168 and 143.5°, respectively). This produces an interlayer shortest distance of 6.42 Å between C3 central carbon atoms.

Slow diffusion of *n*-hexane into an Et_2O solution of radical **1** afforded small crystals of the radical solvate [**1**·$(Et_2O)_3$]. As already also observed in the case of the THF solvates of **1** and **4**, the self-assembled motifs of the diethyl ether solvates are identical, with only small variations in the bond lengths, bond angles, and, by extension, the cell parameters. The main values of dihedral angles, bond lengths, and bond angles are reported in Table 2, in which the values for [**4**·$(Et_2O)_3$] have also been included for purposes of comparison. Because of the sp^2 hybridization of the central carbon (C3), this atom and the three bridgehead carbon atoms (C6) are fixed in the same plane. While the dihedral angles between carboxylic groups and phenyl rings are quite similar, the strongest hydrogen bonds observed in the **4** solvate are weakened. Indeed, the bond length of the O2−H···O5 interaction increases by values of up to 0.1 Å, whereas the bond angle decreases by 14°.[36] Smaller variations are observed in the weak hydrogen bonds involving the CH_2 or CH_3 groups of the Et_2O molecules and the carbonyl groups of **1**. The shortest distance between central carbon atoms is also slightly increased in relation to that observed in the diethyl ether solvate of **4** (6.89 versus 6.42 Å, respectively).

Table 2. Main bond lengths [Å] and bond and dihedral angles [°] found in [**4**·$(Et_2O)_3$] and [**1**·$(Et_2O)_3$].

	[**4**·$(Et_2O)_3$]	[**1**·$(Et_2O)_3$]
Φ[a] [°]	53.9(1)	53.0(1)
C3−$C_{bridgehead}$ [Å]	1.540(3)	1.483(4)
C−C3−C [°]	115.5(2)	119.2(1)
C9-C8-C2-O3 [°]	83.3(3)	83.1(6)
C9-C4-C1-O1 [°]	84.3(5)	85.1(6)
O4−H···O1 [Å][b]	1.78(3) [167(6)]	1.86(3) [163(5)]
O2−H···O5 [Å][b]	1.72(3) (167(6))	1.82(5) (153(8))
O1···H−C11 [Å][b]	2.62 (135)	2.64 (134)
O2···H−C11 [Å][b]	2.60 (165)	2.68 (165)
O1···H−C10 [Å][b]	2.66 (168)	2.71 (166)
O3···H−C13 [Å][b]	2.70 (143)	2.74 (144)

[a] Φ corresponds to the dihedral angle made by the phenyl rings and the reference plane of the molecule. [b] Angles are indicated in parentheses [°].

Molecular and crystal structures of 6: To provide more insight into the correspondence between hydrogen bonding through carboxylic groups and the resulting magnetic properties in radical **1**, the hexaester radical **6** was crystallized and its structure was also analyzed in detail. Crystallographic data are given in Table 1.

The presence of the ester groups completely modifies the solubility properties of radical **6**, a fact that enabled the growth of crystals suitable for X-ray crystal analysis from a mixture of CH_2Cl_2 and *n*-hexane.[37] The hexaester radical crystallizes in the *C*2/c monoclinic space group with four molecules of **6** packed in the unit cell. The molecule presents a twofold rotation axis that passes through Cl5 and the sp^2 central carbon atom C10 (Figure 4). As a result, two of

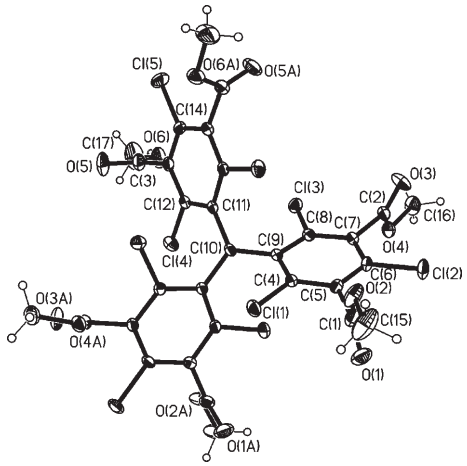

Figure 4. ORTEP representation of radical **6**. Thermal ellipsoids are set at 20% probability (representative atoms labeled).

the aromatic rings are equivalent and the phenyl rings make dihedral angles of 42 and 44° with the reference plane of the molecule. Torsion angles between the methyl ester groups and the phenyl rings to which they are bonded are 88 (C14-C13-C3-O5), 86 (C6-C5-C1-O1), and 72° (C6-C7-C2-O3) in the case of the two aromatic rings that are identical. Four weak hydrogen bonds (C15−H···O3 = 2.35 Å and C15−H···O3 = 152°) per molecule result in the formation of layers along the *ab* plane that have the particularity of being made up only of PTM radicals presenting *P* or *M* helicities (Figure 5). Packing between *P* and *M* layers (AB packing) along the *c* axis is assumed, through four Cl···Cl (Cl4···Cl1 = 3.45 Å) and twelve Cl···O contacts (Cl3···O2 = 3.00, Cl4···O4 = 3.19, and Cl1···O6 = 3.23 Å) per molecule. The shortest distance between central carbon atoms is encountered between *P* and *M* molecules along the *c* axis, with a value of 6.35 Å.

Magnetic properties: X-band ESR spectra of 10^{-4} M solutions of radicals **1** and **6** in Et_2O were obtained. The ESR spectra of the two radicals at room temperature each show one central main line surrounded by four weak satellite lines (Figure 6). These satellite lines originate from the hyperfine coupling between the unpaired electron and the magnetically active ^{13}C nuclei in natural abundance at the α, bridgehead, and *ortho* positions. Experimental spectra can be simulated by using the isotropic hyperfine coupling constants, as reported in Table 3. For purposes of comparison

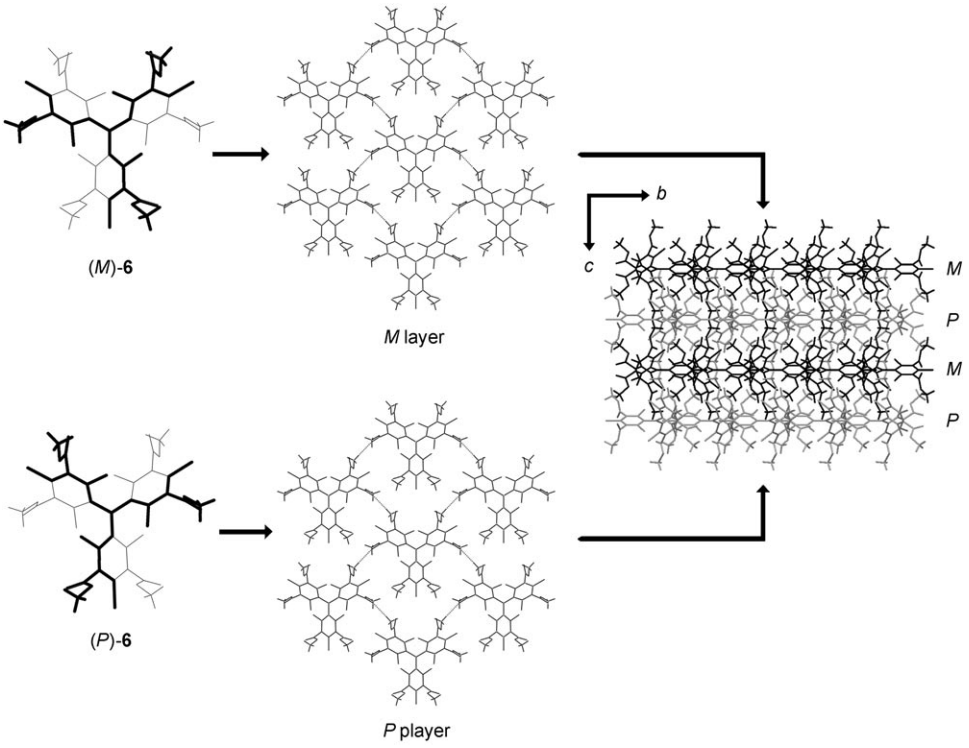

Figure 5. Crystal structure of hexaester **6**. Cl···Cl and Cl···O contacts give rise to the AB packing of weakly hydrogen-bonded *P* and *M* hexaester layers.

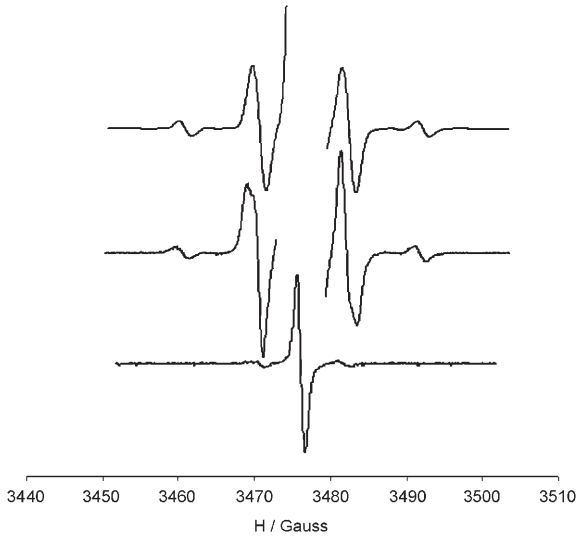

Figure 6. Experimentally measured ESR spectrum (bottom) of a dilute solution of **1** in Et_2O at room temperature ($[C] \approx 10^{-4}$ M). Experimentally measured spectrum (middle) in which the central line has been enlarged in order to observe the satellite lines, together with simulated spectrum (top). Simulation parameters are reported in Table 3.

we also include our previously reported ESR data for carboxylic acid substitution at *para* positions in PTM radicals.[20d,25,26] No significant differences between the *meta*- and the *para*-substituted radicals are observed, which indicates that the changes in the relative positions of the carboxylic groups, together with the increase in their number, do not produce any noticeable change in the spin-density distribution around the PTM core, which in both radicals is mostly localized about the central carbon atoms.[20d,33]

The static magnetic susceptibilities of polycrystalline samples of both the THF and the diethyl ether solvates of **1** and of the hexaester radical **6** were measured between 2 and 300 K on a SQUID susceptometer with an external field of 1000 G. It is important to emphasize that the polycrystalline samples of both solvates of **1** were measured in the presence of a few drops of the mother liquor to avoid fragmentation and loss of crystallinity, which may have disrupted the hydrogen-bonded network and changed the magnetic exchange interactions. At room temperature, the χT product values for all three samples are in good agreement with the theoretical value of 0.375 emu K mol^{-1} expected for uncorrelated $S = 1/2$ systems with $g = 2.0$. With decreasing temperature the χT product values remained constant for all three samples down to very low temperatures, whereupon different behavior patterns were observed. The χT versus T plot for [**1**·THF_6], for instance, exhibits paramagnetic behavior in the 10–200 K temperature range, but with the onset of very weak antiferromagnetic interactions below 10 K. Similar results were obtained for the hexaester radical **6**, which shows paramagnetic behavior from 300 down to 15 K, below which the χT value smoothly decreases, indicating the presence of very weak antiferromagnetic interactions. Both curves were fitted to the Curie–Weiss law, and Weiss constant (θ) values of −0.30 and −0.50 K were obtained for radicals **1** and **6**, respectively. In contrast, the χT versus T plot for [**1**·$(Et_2O)_3$] exhibits an increase in the χT product value at low temperatures, consistent with the presence of intermolecular ferro-

Table 3. Hyperfine coupling constants obtained from simulations of ESR spectra of diluted solutions of radicals **1** and **6**. Values obtained for PTM radicals substituted with one (PTMMC), two (PTMDC), and three (PTMTC) carboxylic acid groups are given for comparison.

PTM radicals	$a_{C\text{-methyl}}$ [Gauss]	$a_{C\text{-}ortho}$ [Gauss]	$a_{C\text{-bridgehead}}$ [Gauss]
PTMMC	29.8	12.7	10.3
PTMDC	29.8	12.5	10.3
PTMTC	29.8	12.6	10.2
1	29.3	13.0	10.5
6	29.3	13.0	10.5

magnetic interactions between different radical units. The θ value obtained from the best fit of experimentally measured data to the Curie–Weiss law yielded a θ value of 0.30 K.

Differences observed for the magnetic interactions in the different solvates of radical **1** are directly related to the structural differences observed in these solvates. The THF solvate of **1** represents the formation of a supramolecular cluster composed of one radical and six THF molecules. Accordingly, the presence of the THF molecules within the supramolecular structure tends to disrupt the formation of a PTM hydrogen-bonded network and consequently the transmission of magnetic interactions mediated by carboxylic groups between the radical units. As a consequence, the presence of weak antiferromagnetic interactions in this solvate is attributable to through-space magnetic interactions, consistently with the lack of direct hydrogen bonds between the PTMHC units and the distance separating the radical centers (7.51 Å).

In the diethyl ether solvate of radical **1**, the structural analysis reveals PTM hydrogen-bonded layers made up of the unusual $R_6^6(48)$ repetitive hexameric units. The existence of direct hydrogen bonds between the PTMHC units in this solvate gives rise to weak ferromagnetic interactions, which are mediated and propagated through the repetitive hydrogen-bonded hexameric units in the layers.

The role played here by the hydrogen-bonded carboxylic groups in the formation of hydrogen-bonded layers and in the transmission of magnetic interactions is highlighted by comparing the structural and magnetic properties of [**1**·$(Et_2O)_3$] with those of methyl ester **6**. The latter compound exhibits a close-packed, guest-free structure, most probably due to the presence of methyl ester groups that do not have the crucial ability to form strong directional intermolecular interactions. The presence of short Cl···Cl contacts, which are well known to yield antiferromagnetic interactions in PTM derivatives, may be argued to explain the magnetic behavior found for this radical.

Attempts to obtain solvent-free structures—crystallizations from nitric acid: The presence of weak but ferromagnetic interactions propagating along the layers of the diethyl ether solvate of radical **1** motivated us to increase the structural dimensionality of the hydrogen-bonded network to a 3D hydrogen-bonded form, which may potentially exhibit magnetic ordering. The main limitation to overcome in achieving this target was the use of polar solvents, otherwise necessary to dissolve the sample, but with the potential to disrupt the hydrogen-bonded supramolecular network because of their competing interactions for hydrogen bonds. Initially, to avoid the use of solvents that might become involved in the formation of the hydrogen bonds, different solvents, such as diethyl ether or diisopropyl ether, and several crystallization trials (such as slow diffusion or slow evaporation) were carried out. All these trials failed, in most cases resulting in the recovery of amorphous solids.

The difficulty involved in obtaining pure carboxylic acid hydrogen-bonded networks with polycarboxylic acid compounds is a general trend, as was confirmed after a thorough crystallographic search on the Cambridge Crystallographic Database and other different bibliographic sources. This quest revealed the existence of only a limited number of tetra- (or more) carboxylic acid-substituted scaffolds[7a–e,27,28] that crystallize without disruption of the direct hydrogen bonds between carboxylic acid groups by solvent molecules. In the cases of compounds **7** and **8**, for instance, the formation of $R_2^2(8)$ dimers between carboxylic groups created interpenetrated, hydrogen-bonded, diamondlike lattices. Crystals of these molecules were grown by a gas-phase neutralization technique, that is, the diffusion of HCl vapor into saturated solutions of the tetracarboxylates of **7** and **8**.[7a,b] With compound **9** a hydrogen-bonded layer was obtained from a crystallization from concentrated nitric acid.[27a]

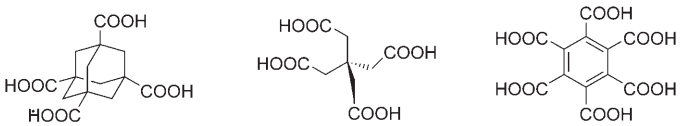

With compounds **1** and **4**, HCl gas diffusion failed to provide crystals of sufficient quality to solve the X-ray crystal structure. However, crystallization of compound **4** from concentrated nitric acid (65%) at 100°C afforded robust, colorless prisms of solvate [**4**·$(H_2O)_{1.5}$]. This solvate crystallizes in the $P\text{-}42_1c$ tetragonal space group with eight molecules of hexa-acid and twelve molecules of water in the unit cell. The three aromatic rings here are different from those in the THF and diethyl ether solvates of the same compound, being twisted by angles of 48, 48, and 59° with respect to the reference plane of the molecule (Figure 7). Moreover, the carboxylic acid groups are also twisted by angles of between 82 and 88°, owing to the presence of the bulky chlorine atoms at the *ortho* positions. Main distances and bond

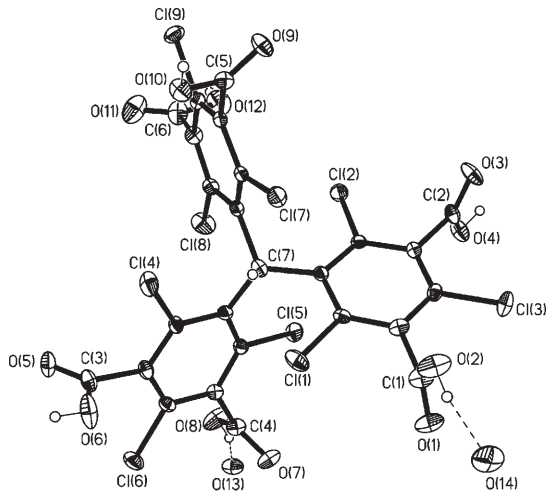

Figure 7. ORTEP representation of the PTM molecule of **4** found in [**4**·$(H_2O)_{1.5}$]. Thermal ellipsoids are set at 20% probability and symmetry-related solvent molecules have been omitted for clarity (representative atoms labeled).

angles for [**4**·$(H_2O)_{1.5}$] are reported in Table 4, with hydrogen bonds involving water molecules being described by O···O distances.

As far as the supramolecular packing is concerned, four hexa-acid molecules of alternating *P* and *M* helicities are associated through two O10–H···O7 and two O6–H···O3 hydrogen bonds to form $R_4^4(48)$ tetramers in the *ab* plane (Figure 8a). The resulting polar nest is filled by two water molecules that form two O2–H···O14 and two O14–H···O11 hydrogen bonds with PTM molecules. In addition, these two water molecules are linked through an O14–H···O14 hydrogen bond. Packing of a similar supramolecular unit takes place along the *c* axis, through four O12–H···O5 hydrogen bonds (Figure 8b). The distance between water molecules belonging to different dimers in the resulting polar box is 3.38 Å. Packing of the boxes takes place through O4–H···O1 hydrogen bonds, generating infinite supramolecular square towers running along the *c* axis (Figure 8c). Each molecule of **4**, located in the corner of the square, is involved in the formation of similar motifs, resulting in a chessboardlike arrangement of the towers when the structure is viewed along the *c* axis (Figure 8d). This kind of assembly generates polar channels that are filled by isolated water molecules, separated from one another by 7.63 Å (Figure 8e). They are held in the network by four hydrogen bonds with the carboxylic acid groups (two O8–H···O13 and two O13–H···O9). All these motifs are reinforced by Cl···Cl and Cl···O short contacts (see Table 4). Platon calculations revealed that the structure of this solvate possesses an accessible volume close to 8.5% when the water molecules are omitted, corresponding to a solvent-accessible volume of 568.1 Å^3 with respect to the volume of the total unit cell (6564.0 Å^3).[38]

Table 4. Main bond lengths [Å] and bond angles [°] encountered for hydrogen bonds and short contacts in [**4**·$(H_2O)_{1.5}$].

	$d_{H\cdots O}$ [Å]	$d_{O\cdots O}$ [Å]	Bond angles [°]
O2–H···O14	1.77	2.592(9)	170.4
O4–H···O1	1.89	2.656(6)	153.5
O6–H···O3	1.96	2.720(6)	150.9
O8–H···O13	1.86	2.628(6)	153.9
O10–H···O7	1.86	2.666(6)	163.1
O12–H···O5	1.97	2.737(7)	152.9
O13–H···O8	–	2.629(6)	–
O13–H···O9	–	2.746(6)	–
O14–H···O11	–	2.67(1)	–
O14–H···O14	–	2.69(2)	–
	$d_{Cl\cdots Cl}$ [Å]	$d_{Cl\cdots O}$ [Å]	
Cl1···Cl9	3.32	–	–
Cl8···Cl9	3.41	–	–
Cl5···O6	–	2.98	–
Cl6···O9	–	3.13	–
Cl9···O8	–	3.12	–

The similarities already found for the THF and diethyl ether solvates of **1** and **4**, together with the obtaining of a porous material by crystallization of **4** from nitric acid, prompted us to crystallize radical **1** from the same acid: if successful, this could have led us to the obtaining of a pure organic porous material with a 3D hydrogen-bonded structure similar to the water solvate of **4**, with foreseeable potential magnetic properties. However, and in spite of the fact that the fully chlorinated PTM radical had already been shown to be stable in concentrated nitric acid over several days,[39] **1** was oxidized with nitric acid to give the corresponding diamagnetic fuchsone **10** (see Scheme 2), probably

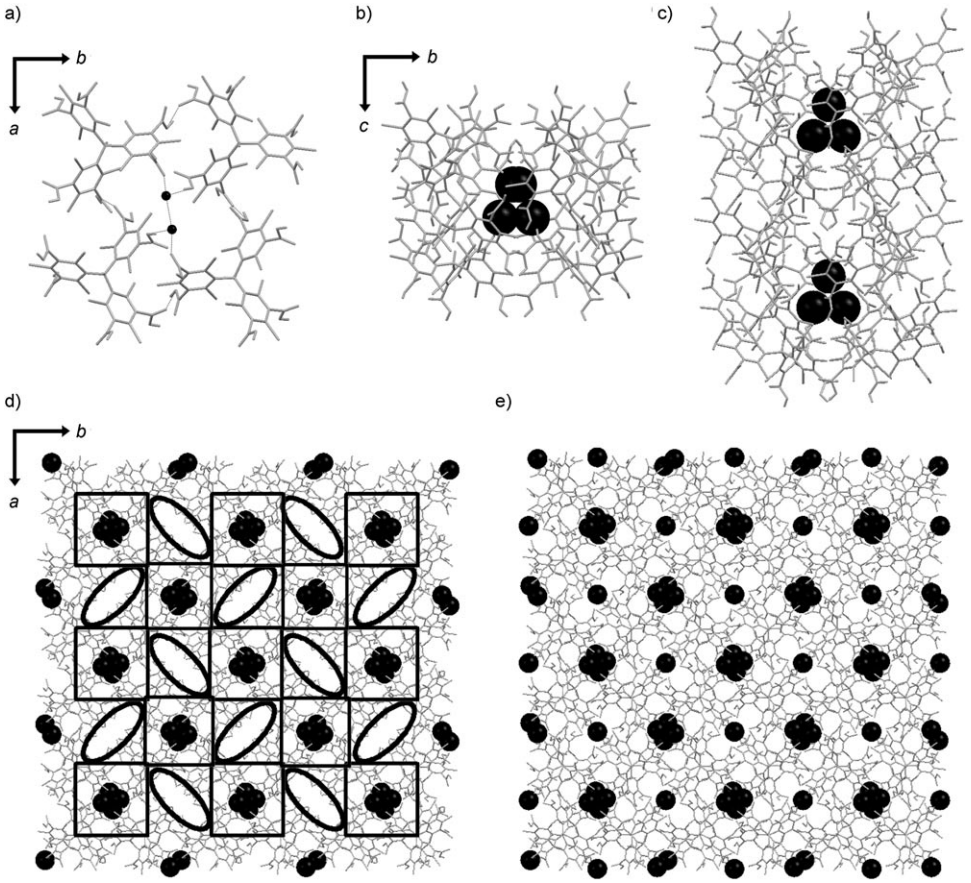

Figure 8. Crystal structure of [**4**·$(H_2O)_{1.5}$]. a) $R_4^4(48)$ tetramer "filled" with two water molecules and b) polar box containing water resulting from the packing of two tetramers. c) Supramolecular tower running along the *c* axis. d) Chessboardlike arrangement of the supramolecular towers (squares), producing polar channels (surrounded) filled by isolated water guest molecules (e). Water molecules are represented as spheres for clarity.

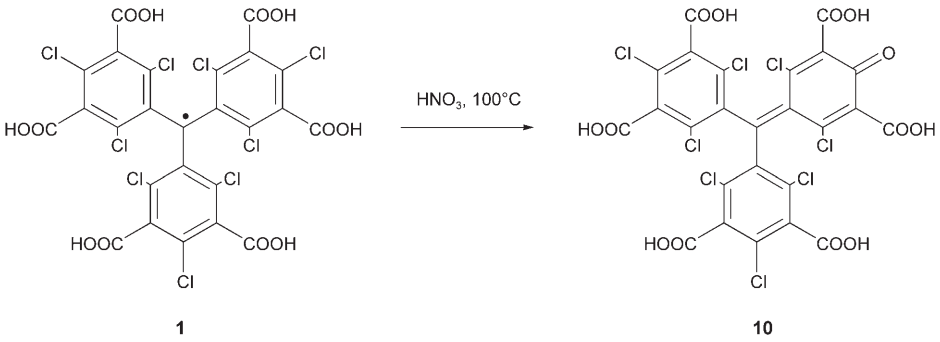

Scheme 2.

as a result of the good solubility of this compound in nitric acid at high temperatures, which contrasts with the low solubility of the fully chlorinated PTM radical.[40]

Compound **10** was obtained as dark orange blocks that crystallize in the orthorhombic space group with eight molecules of fuchsone packed in the unit cell. Cell parameters are reported in Table 1 and an ORTEP drawing for compound **10** is shown in Figure 9. Fuchsone **10** exhibits a two-

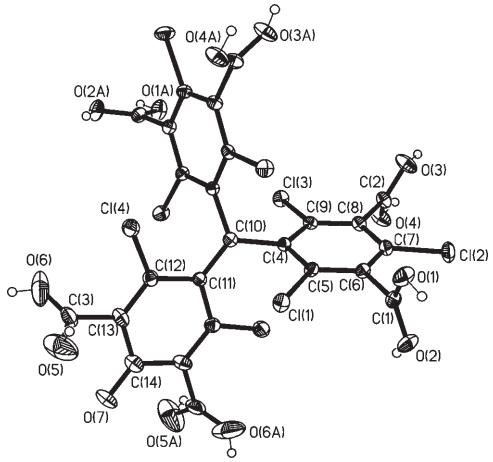

Figure 9. ORTEP representation of the fuchsone **10** with occupancy of 0.5 for each hydrogen atom (positional disorder). Thermal ellipsoids are set at 20% probability and symmetry-related solvent molecules have been omitted for clarity (representative atoms labeled).

fold rotation axis that passes through the ketone oxygen atom (O7) and the central sp^2 carbon atom (C10). As a consequence, the two aromatic rings substituted by three chlorine atoms are equivalent. In comparison with the THF and diethyl solvates of **1**, in which the hybridization state of the central carbon atom is also sp^2, the presence of a double bond between C10 and C11 is translated into a very low dihedral angle for the quinone ring, which is twisted by 28° with respect to the reference plane of the molecule, whereas the two other aromatic rings present dihedral angles of 57° with the reference plane.[41] The carboxylic acid groups on the trichlorinated rings are twisted by angles of 81 (C7-C6-C1-O2) and 70° (C7-C8-C2-O3). The latter value is quite low in relation to those found in **1** and its precursors (between 80 and 88°), despite the presence of the chlorine atoms at *ortho* positions. A 1:1 disorder is observed for each carboxylic acid group, with apparent equivalent C–O bond lengths (around 1.25 Å). These bond lengths are slightly shortened in the carboxylic groups on the quinone ring (around 1.19 Å), probably because of better conjugation with the six-membered ring arising from the lower dihedral angles encountered for these groups. As a consequence of this disorder, the hydrogen atoms are also disordered, showing a 0.5 occupancy for those bounded to the oxygen atoms of each carboxylic group. Because of such disorder, the hydrogen bonds are described below only in terms of the O···O distances.

The three different types of carboxylic acid groups involved in the three different supramolecular motives (I, II, and III) are shown in Figures S1 and S2 in the Supporting Information. The $R_2^2(8)$ dimers involving the carboxylic groups that contain C2 (pattern I, O3···O4 = 2.64 Å) give rise to the formation of helical chains running in the *ac* plane (Figure 10).

Two different helicities are obtained, depending on the conformation adopted by **10**, giving rise to *M* and *P* chains formed by (*M*)-**10** and (*P*)-**10** molecules, respectively. These chains associate to give *M*- and *P*-layers in a peculiar zigzag supramolecular pattern (II, Figure S1) that involves the carboxylic acid groups containing C2 and the ketone oxygen atom (O7). These supramolecular polymeric chains involve O7 and two O5 oxygen atoms as potential hydrogen bond acceptors (O5···O5 = 2.64 Å and O7···O5 = 2.80 Å).

The 1:1 disorder observed for the two carboxylic acid groups and the hydrogen atoms connected to them, together with the two O···O distances encountered (which are short enough to make possible hydrogen bonds), did not enable us to determine the nature of the supramolecular motif.[42] "Interpenetration" of the *M* and *P* layers (Figure 11) occurs through Cl···O short contacts (two per molecule, Cl1···O3 = 3.05 Å) and π–π interactions between C=O groups and aromatic or quinone rings (O3···C14 = 3.15 Å and O7···C9 = 3.04 Å). *P*/*M* interpenetrated layers are connected through hydrogen-bonded polymeric chains running along the *ab* plane involving both (*M*)- and (*P*)-**10** molecules (III, Figure S2). The O···O distances (O1···O1 = 2.63 Å, O2···O2 = 2.70 Å), together with geometrical factors (C1-O1-O1-C1 = 119° and C1-O2-O2-C1 = 180°),[43] enable this chain to be described as one more example of the very rare *syn-anti* catemer-type motif.[44]

Although diamagnetic and nonporous, the structure obtained for compound **10** does provide an illustration of how subtle modifications in the geometry of the PTM-based

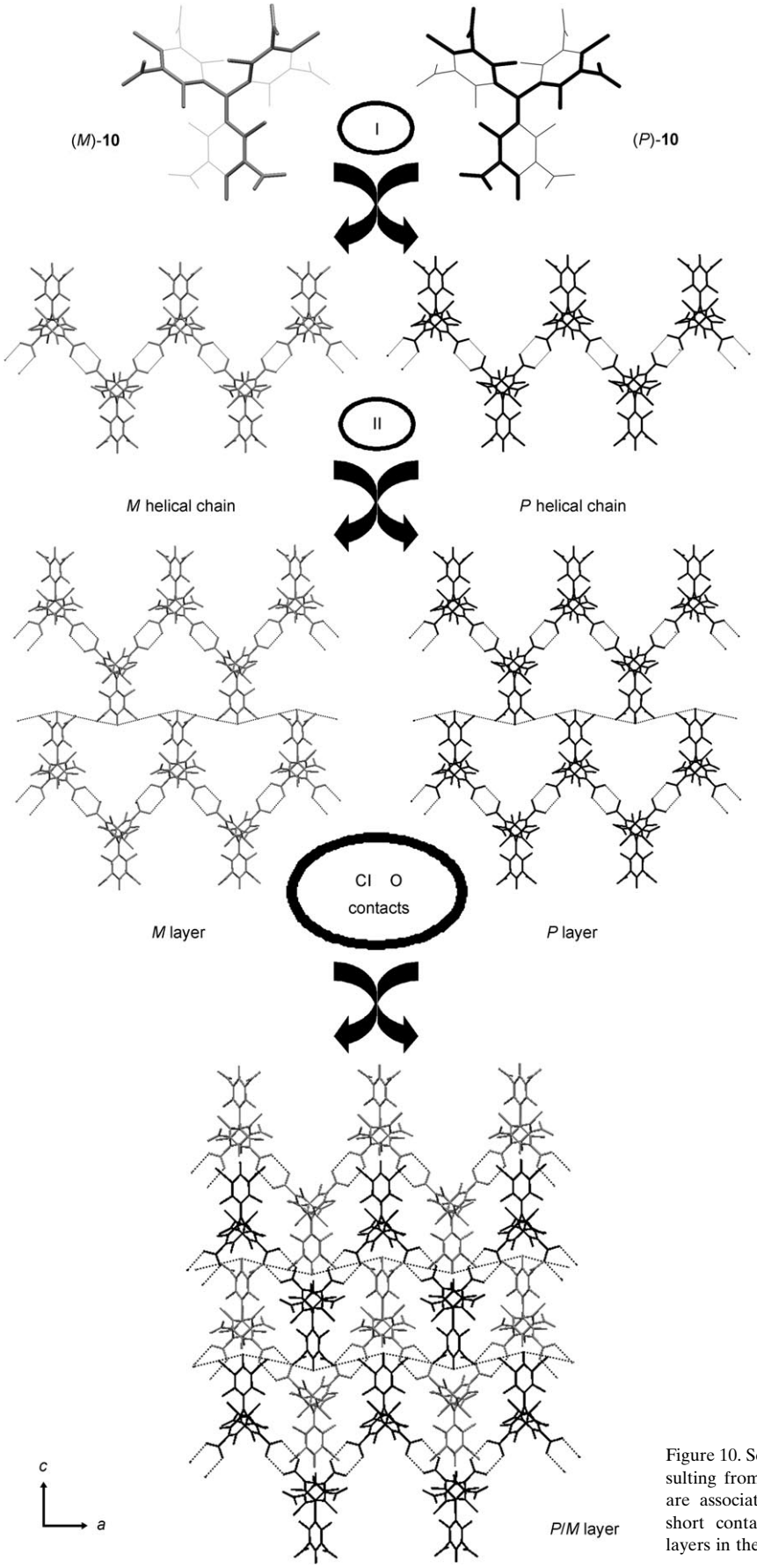

Figure 10. Self-assembly of **10**. Helical *P* and *M* chains, resulting from $R_2^2(8)$ dimer associations of (*P*)- and (*M*)-**10**, are associated to form *P* and *M* layers. Chlorine–oxygen short contacts enable the "interpenetration" of the two layers in the *ac* plane.

tecton could give rise to dramatic changes in the self-assembly of the molecules and in the resulting final structures. Indeed, **10** possesses a rigid core with a well-defined, three-bladed, helix geometry surrounded by six *meta*-carboxylic acid groups, similar to that reported for compounds **1** and **4**. The most important changes in the tecton relate to the formation of the fuchsone ring during the recrystallization, which is mainly reflected in a modification of the helicity angle, the replacement of one bulky *para* chlorine atom by a less voluminous and potential hydrogen-bond acceptor oxygen atom—of the ketone group—and by the dihedral angle modifications for the carboxylic groups close to this oxygen atom. Noteworthy is the presence of the unusual moiety involving three hydrogen-bond acceptors and two hydrogen-bond donors that gives rise both to the formation of layers and to the formation of the unusual *syn-anti* catemer-type motif that connects the *P*/*M* interpenetrated layers to create the 3D, solvent-free, hydrogen-bonded structure (Figure 12).

If the hydrogen bonds linking the *P* and *M* molecules are neglected in this motif, the close-packed, guest-free structure may be described as the result of the interpenetration of a nanoporous framework made of *P* molecules of **10** with the corresponding nanoporous framework made of *M* molecules of **10**. Even though the structure is a nonporous structure, as a result of better shape complementarities than

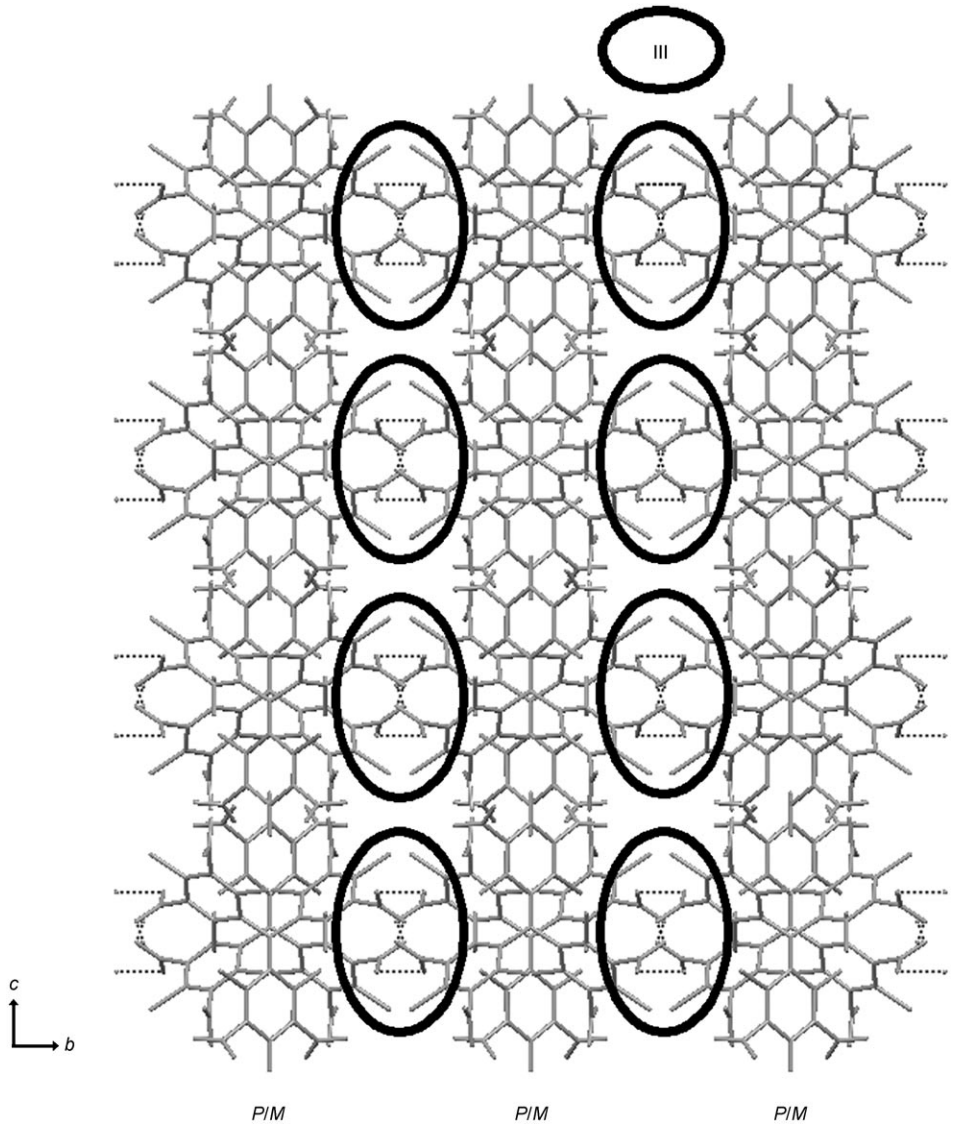

Figure 11. Self-assembly of (*P*/*M*)-interpenetrated layers.

in the corresponding (*P*)- and (*M*)-PTM units, it clearly shows that the tectons based on the hexacarboxylic acid PTM are promising candidates for the design of porous 3D hydrogen-bonded networks. From a supramolecular and a magnetic point of view, the challenge is now to find appropriate conditions to avoid the disruption of the network by solvent molecules, interpenetration, or the chemical alteration of the radical.

Conclusion

In this article we have reported the detailed synthesis of the first example of a PTM radical substituted with six carboxylic acid groups at *meta* positions, compound **1**, which to the best of our knowledge is the first example of a paramagnetic hexacarboxylic acid. This molecule was obtained in good yields by an original six-step methodology. Study of the self-assembly of this 3D, six-connecting organic building block and of its precursor **4** revealed that it is possible, through a slight tuning of the crystallization conditions, to control the structural dimensionality and to go from 0 to 2D structures, in which the association of radicals through direct hydrogen bonds to form layers gives rise to the presence of weak ferromagnetic intermolecular interactions between radicals. Attempts to produce 3D hydrogen-bonded structures were performed by recrystallizion of **4** and **1** in concentrated nitric acid. While a 3D hydrogen-bonded structure presenting polar boxes and channels was obtained with **4**, a completely different structure was obtained with radical **1**, as it was oxidized in situ to the corresponding fuchsone **10** during the recrystallization process. The structural analysis we performed on this byproduct clearly illustrates how subtle changes in the molecular structure of a tecton may induce dramatic changes both in the synthons that are formed and also in the resulting final structure. Crystallization attempts to find appropriate conditions that will enable us to avoid the disruption of the network by solvent molecules, interpenetration, and the chemical alteration of the radical are currently in progress in our laboratory. Our efforts are also being addressed towards the use of molecule **1** as an open-shell organic ligand of paramagnetic metal ions, with the idea of building robust and 3D magnetic metal-organic frameworks.[45]

Experimental Section

X-ray measurement and structure determination: Data collection was performed on a Nonius Kappa CCD with graphite-monochromatized $Mo_{K\alpha}$ radiation ($\lambda = 0.71073$ Å) and a nominal crystal to area detector distance of 36 mm. Intensities were integrated by using DENZO and scaled with SCALEPACK. Several scans in the φ and ω directions were made to increase the number of redundant reflections, which were averaged in the refinement cycles. This procedure replaces an empirical ab-

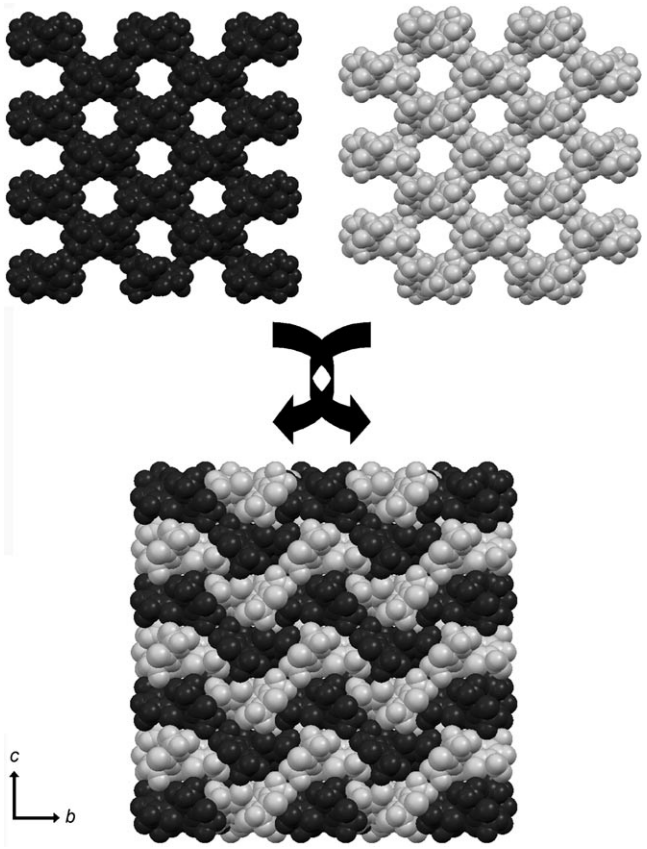

Figure 12. *P* and *M* nanoporous frameworks giving rise to the close-packed, guest-free structure of **10**.

sorption correction to a good approximation. The structures were solved by direct methods (SHELXS86) and refined against F^2 (SHELX97). The *R* value of [**1**·THF$_6$] is slightly higher, the result of low diffraction from small crystal size (the volume was around 10 times smaller than that of [**4**·THF$_6$]).

All non-hydrogen atoms were refined with anisotropic displacement parameters, except in disordered THF in [**1**·THF$_6$]. Hydrogen atoms attached to carbon atoms were calculated and refined with isotropic displacement parameters 1.2 or 1.5 times higher than the value of their carbon atoms. Hydrogen atoms were found at most carboxylic acid groups and were refined isotropically with bond restraints (d_{OH} = 0.85 Å), except in the case of [**4**·(H$_2$O)$_{1.5}$], in which hydrogen atoms were not exactly localized in the same positions and were therefore refined in calculated positions, whilst hydrogen atoms of water molecules were omitted. Because of the disorder of hydrogen atoms in **10** the treatment of their refinement was mixed, with refinement in found and calculated positions (see below).

There are different types of disorder in the structures. In the THF and water solvates of **4** the central carbon atoms are positionally disordered in the opposite direction to the plane of the three attached phenyl carbon atoms in ratios of 2:1 and 3:2, respectively. Further positional disorder occurs in the water molecule of [**4**·(H$_2$O)$_{1.5}$], where O14 and O14 A have a ratio of 3:1 and the position of O14 A in the structure is not discussed. The THF molecules in the THF solvates of **1** and **4** are also positionally disordered. In **4** the first THF molecule (C10–C13–O5) is slightly disordered, and only the oxygen atom was refined in two positions, whereas the second THF molecule (C14–C17–O6) was completely disordered into two positions. The ratio of the two THF molecules is around 5.6:1 and the minor part is not included in the structural discussion. In **1** the first THF molecule is only slightly disordered and the disorder was not solved, whereas the second one (C14–C17–O6) was completely disordered in a 1:1 ratio with partially overlying carbon atoms. This THF molecule could only be refined with bond restraints and isotropic displacement parameters. Finally, all the oxygen atoms of the carboxylic acid groups of **10** are 1:1 positionally disordered, with the hydroxy oxygen atoms overlaying exactly with the carbonyl oxygen atoms of the other part, so hydrogen atoms are connected to each oxygen atom with occupancies of 0.5. The hydrogen atoms at O2 and O5 were found in these positions and were refined with bond restraints; the other hydrogen atoms at O1, O3, O4, and O6 were also found, but were refined in calculated positions.

CCDC 602916–602920, 276958, and 276959 contain the supplementary crystallographic data for this paper. These data can be obtained free of charge from the Cambridge Crystallographic Data Centre via www.ccdc.cam.ac.uk/data_request/cif.

Materials and methods: Solvents were distilled before use. In particular, Et_2O was dried over sodium/benzophenone and distilled under argon. All the commercial reagents were purchased from Aldrich and used as received. Chromatography was performed on SDS silica gel ($60F_{254}$). ^{1}H and ^{13}C NMR spectra were recorded on a Bruker ARX 300 spectrometer (^{1}H NMR recorded at 300 MHz, ^{13}C NMR recorded at 300 MHz), FTIR spectra on a Perkin–Elmer Spectrum One spectrometer, and the UV/visible spectra on a VARIAN Cary 5 instrument. Direct current (dc) magnetic susceptibility measurements were carried out on a Quantum Design MPMS SQUID susceptometer with a 55 kG magnet operating in the range of 4–320 K. All measurements were collected in a field of 10 kG. Background correction data were collected from magnetic susceptibility measurements of the holder capsules. Diamagnetic corrections estimated from the Pascal contents were applied to all data for determining the molar paramagnetic susceptibilities of the compounds. ESR spectra were recorded on a Bruker ESP-300E spectrometer operating in the X-band (9.3 GHz). The signal-to-noise ratio was improved by accumulation of scans with use of the F/F lock accessory to guarantee high-field reproducibility. Precautions were taken to avoid undesirable spectral line-broadening, such as that arising from microwave power saturations and magnetic field over-modulation. To avoid dipolar broadening, the solutions were carefully degassed three times by using vacuum cycles with pure Ar. The g values were determined against the DPPH standard (g = 2.0030).

Compound 2:[31a] A mixture of 1,3,5-trichlorobenzene (10.14 g, 55.9 mmol, 9 equiv), anhydrous chloroform (0.5 mL, 6.2 mmol, 1 equiv), and aluminum chloride (0.91 g, 6.8 mmol, 1.1 equiv) was heated at 80 °C for 2.5 h in a glass pressure vessel. The mixture was then poured onto ice/hydrochloric acid (1 N) and extracted several times with chloroform. The organic phase was dried over anhydrous sodium sulfate and the solvent was removed. The excess of 1,3,5-trichlorobenzene was removed over silica gel by using pure hexane as the eluent to give **2** as a white powder in 70 % yield (2.4 g, 4.34 mmol). M.p. 246–248 °C (lit.[31a] m.p. 246–248 °C); ^{1}H NMR (CCl_4/D_2O) δ = 6.9 (s, 1 H), 7.1 (d, J = 2 Hz, 3 H; H_{arom}), 7.2 ppm (d, J = 2 Hz, 3 H; H_{arom}); IR (KBr): $\tilde{\nu}$ = 3120, 3080, 2905, 1570, 1540, 1430, 1420, 1365, 1245, 1185, 1170, 1140, 1130, 895, 854, 815, 800, 670, 570, 440 cm^{-1}.

Compound 3:[31b] A mixture of compound **2** (1.8 g, 3.25 mmol, 1 equiv), anhydrous chloroform (140 mL), and aluminum chloride (0.66 g, 4.95 mmol, 1.5 equiv) was heated at 80 °C for 24 h. The mixture was then poured onto ice/hydrochloric acid (1 N) and extracted several times with chloroform. The organic phase was dried over anhydrous sodium sulfate and the solvent was removed. The crude product was purified over silica gel by using $CHCl_3$/hexane 1:3 as the eluent to give **3** as a white powder in 70 % yield (2.39 g, 2.27 mmol). M.p. 250 °C (decomp); ^{1}H NMR (CD_2Cl_2): δ = 6.9–7.2 (m, 1 H), 7.6–7.8 ppm (m, 6 H); IR (KBr): $\tilde{\nu}$ = 3044, 1532, 1373, 1274, 1223, 1043, 1007, 788, 721, 685, 582, 437 cm^{-1}.

Compound 4: Compound **3** (500 mg, 0.47 mmol) was mixed with oleum (20 %) and the mixture was heated at 150 °C for 24 h. The final solution was cooled and poured onto cracked ice, the aqueous phase was saturated with brine and extracted with Et_2O, and the organic phase was con-

centrated and extracted with aqueous sodium carbonate. The resulting aqueous phase was acidified, saturated with brine, and extracted several times with Et_2O. The organic phase was dried over anhydrous sodium sulfate and the solvent was removed. The crude product was dissolved in Et_2O (5 mL) and precipitated several times in hexane to give **4** as a white powder in 75% yield (280 mg, 0.36 mmol). ^{1}H NMR ([D$_6$]DMSO): $\delta =$ 5.5 (brs, 6H), 6.8 ppm (s, 1H); ^{13}C NMR ([D$_6$]DMSO): $\delta = 55.3$, 130.8, 136.6, 137.4, 138.6, 140.3, 141.5, 168.9 ppm; IR (KBr): $\tilde{\nu} = 3500$–2500, 1710, 1540, 1355, 1299, 1230, 1203, 1119, 1036, 968, 816, 731, 605, 471 cm^{-1}; elemental analysis (%) calcd for $C_{25}H_7Cl_9O_{12}$: C 36.69, H 0.86; found: C 36.65, H 0.89.

Compound 5: An Et_2O solution of freshly prepared diazomethane (0.4 M, 16 mL, 6.43 mmol, 7 equiv) was slowly added at room temperature to a solution of hexa-acid **4** (750 mg, 0.92 mmol, 1 equiv) in freshly distilled Et_2O (100 mL). The mixture was stirred for 8 h and the excess of diazomethane was removed by bubbling nitrogen. The organic phase was washed with aqueous sodium carbonate, dried over anhydrous sodium sulfate, and the solvent was evaporated. The remaining solid was purified over silica gel by using pure dichloromethane as an eluent to give **5** as a white powder in 80% yield (670 mg, 0.74 mmol). M.p. 192 °C (decomp); ^{1}H NMR ([D$_6$]DMSO): $\delta = 3.9$ (s, 9H), 4.0 (s, 9H), 6.9 ppm (s, 1H); ^{13}C NMR ([D$_6$]DMSO): $\delta = 50.6$, 53.1, 53.2, 128.5, 133.7, 133.8, 134, 134.9, 135, 163.4, 163.5 ppm; IR (KBr): $\tilde{\nu} = 3006$, 2955, 2919, 2850, 1744, 1555, 1436, 1378, 1327, 1253, 1182, 1112, 1042, 991, 935, 891, 833, 822, 807, 785, 765, 671, 645, 620, 560, 543, 490 cm^{-1}; elemental analysis (%) calcd for $C_{31}H_{19}Cl_9O_{12}$: C 41.25, H 2.12; found: C 41.25, H 2.18.

Radical 6: A tetrabutylammonium hydroxide solution in methanol (1.75 mL, 0.26 mmol, 1.2 equiv) was added to a solution of **5** (200 mg, 0.22 mmol, 1 equiv) in freshly distilled THF (50 mL). The mixture was stirred for 1 h, and *p*-chloranil (220 mg, 0.88 mmol, 4 equiv) was added as a solid. After 2 h of stirring, the solvent was removed to yield a purple solid that was purified over a preparative silica-gel plate by using pure CH_2Cl_2 as an eluent. The pure radical **6** was recovered as a red solid, in 80% yield (160 mg, 0.18 mmol). M.p. 186 °C (decomp); IR (KBr): $\tilde{\nu} =$ 2955, 2924, 2853, 1747, 1556, 1454, 1435, 1379, 1328, 1237, 1177, 1116, 987, 932, 888, 824, 804, 763, 740, 641, 615, 547, 484 cm^{-1}; UV/Vis (THF): λ_{max} (ε) = 378 (30050), 545 nm (775 mol^{-1} dm^3 cm^{-1}); elemental analysis (%) calcd for $C_{31}H_{18}Cl_9O_{12}$: C 41.30, H 2.01; found: C 41.36, H 1.94.

Radical 1: Compound **5** (160 mg, 0.18 mmol) was mixed with concentrated sulfuric acid and the mixture was heated at 90 °C for 12 h. The final solution was cooled and poured onto cracked ice, the aqueous phase was saturated with brine and extracted with Et_2O. The organic phase was concentrated and extracted with aqueous sodium carbonate. The resulting aqueous phase was acidified, saturated with brine, and extracted several times with Et_2O. The organic phase was dried over anhydrous sodium sulfate, the solvent was removed, and the crude product was dissolved in Et_2O (5 mL) and precipitated several times in hexane to give **1** as a red powder in 90% yield (130 mg, 0.16 mmol). IR (KBr): $\tilde{\nu} = 3500$–2500, 1715, 1631, 1538, 1439, 1340, 1246, 1120, 1064, 974, 928, 900, 830, 812, 741, 681, 622, 583, 487 cm^{-1}; UV/Vis (THF): λ_{max} (ε) = 378 (30150), 545 nm (820 mol^{-1} dm^3 cm^{-1}); elemental analysis (%) calcd for $C_{25}H_6Cl_9O_{12}$: C 36.74, H 0.74; found: C 36.70, H 0.77.

Compound 10: IR (KBr): $\tilde{\nu} = 3500$–2500, 1716, 1666, 1596, 1550, 1478, 1384, 1350, 1250, 1123, 929, 885, 711, 622 cm^{-1}; UV/Vis (DMSO): λ_{max} (ε) = 444 nm (20090 mol^{-1} dm^3 cm^{-1}); elemental analysis (%) calcd for $C_{25}H_6Cl_8O_{13}$: C 36.74, H 0.74; found: C 36.67, H 0.80.

Acknowledgements

This work was supported by the EU under a Marie Curie Research Training Network contract ("QuEMolNa" number MCRTN-CT-2003-504880) and NOE MAGMANET (contract 515767-2), as well as by MEC (DGI, Spain) under project MAT2003-04699. N.R. thanks the MCRTN for its postdoctoral contract and D.M. is grateful to the Generalitat de Catalunya for a postdoctoral grant. We would also like to thank Dr. Jose Vidal-Gancedo for his help with the EPR spectra.

[1] a) G. R. Desiraju, *Crystal Engineering: The Design of Organic Solids*, Elsevier, Amsterdam, **1989**; b) P. Langley, J. Hulliger, *Chem. Soc. Rev.* **1999**, *28*, 279–291; c) M. Hollingsworth, *Science* **2002**, *295*, 2410–2413; L. Perez-Garcia, D. Amabilino, *Chem. Soc. Rev.* **2002**, *31*, 342–356; d) J. Veciana, H. Iwamura, *MRS Bull.* **2000**, *25*, 41–51; e) S. Yagai, T. Karatsu, A. Kitamura, *Chem. Eur. J.* **2005**, *11*, 4054–4063.

[2] a) J. MacDonald, G. Whitesides, *Chem. Rev.* **1994**, *94*, 2383–2420; b) D. Lawrence, T. Jiang, M. Levett, *Chem. Rev.* **1995**, *95*, 2229–2260.

[3] a) T. Tanaka, T. Tasaki, Y. Aoyama, *J. Am. Chem. Soc.* **2002**, *124*, 12453–12462; b) R. Melendez, A. Hamilton, *Top. Curr. Chem.* **1998**, *198*, 97–129.

[4] a) B. Moulton, M. Zaworotko, *Chem. Rev.* **2001**, *101*, 1629–1658; b) B. Gong, C. Zheng, E. Skrzypczak-Jankun, Y. Yan, J. Zhang, *J. Am. Chem. Soc.* **1998**, *120*, 11194–11195; c) N. Malek, T. Maris, M.-E. Perron, J. D. Wuest, *Angew. Chem.* **2005**, *117*, 4089–4093; *Angew. Chem. Int. Ed.* **2005**, *44*, 4021–4025; d) C. Krishnamohan Sharma, A. Clearfield, *J. Am. Chem. Soc.* **2000**, *122*, 4394–4402.

[5] D. Philp, J. Fraser Stoddart, *Angew. Chem.* **1996**, *108*, 1242–1286; *Angew. Chem. Int. Ed. Engl.* **1996**, *35*, 1154–1196.

[6] G. R. Desiraju, *Angew. Chem.* **1995**, *107*, 2541–2558; *Angew. Chem. Int. Ed. Engl.* **1995**, *34*, 2311–2327.

[7] To the best of our knowledge, most of the purely organic 3D assemblies reported so far are based on four-connecting molecular building blocks with Td symmetry, such as adamantane, tetraalkyl- or -arylmethane, silane, or stannane, and twisted bipyrazole or biphenyl derivatives. See: a) O. Ermer, A. Eling, *Angew. Chem.* **1988**, *100*, 856–860; *Angew. Chem. Int. Ed. Engl.* **1988**, *27*, 829–833; b) O. Ermer, *J. Am. Chem. Soc.* **1988**, *110*, 3747–3754; c) P. Holy, J. Zavada, I. Cisarova, J. Podlaha, *Angew. Chem.* **1999**, *111*, 393–395; *Angew. Chem. Int. Ed.* **1999**, *38*, 381–383; d) P. Holy, J. Zavada, I. Cisarova, J. Podlaha, *Tetrahedron: Asymmetry* **2001**, *12*, 3035–3045; e) J. Moorthy, R. Natarajan, P. Venugopalan, *J. Org. Chem.* **2005**, *70*, 8568–8571; f) X. Wang, M. Simard, J. D. Wuest, *J. Am. Chem. Soc.* **1994**, *116*, 12119–12120; g) D. S. Reddy, D. Craig, G. R. Desiraju, *J. Am. Chem. Soc.* **1996**, *118*, 4090–4093; h) P. Brunet, M. Simard, J. D. Wuest, *J. Am. Chem. Soc.* **1997**, *119*, 2737–2738; i) D. S. Reddy, T. Dewa, K. Endo, Y. Aoyama, *Angew. Chem.* **2000**, *112*, 4436–4438; *Angew. Chem. Int. Ed.* **2000**, *39*, 4266–4268; j) R. Thaimattam, C. K. Sharma, A. Clearfield, G. R. Desiraju, *Cryst. Growth Des.* **2001**, *1*, 103–106; k) J.-H. Fournier, T. Maris, M. Simard, J. D. Wuest, *Cryst. Growth Des.* **2003**, *3*, 535–540; l) I. Boldog, E. Rusanov, J. Sieler, S. Blaurock, K. Domasevitch, *Chem. Commun.* **2003**, 740–741; m) J.-H. Fournier, T. Maris, J. D. Wuest, W. Guo, E. Galoppini, *J. Am. Chem. Soc.* **2003**, *125*, 1002–1006; n) H. Sauriat-Dorizon, T. Maris, J. D. Wuest, *J. Org. Chem.* **2003**, *68*, 240–246; o) J.-H. Fournier, T. Maris, J. D. Wuest, *J. Org. Chem.* **2004**, *69*, 1762–1775; p) O. Saied, T. Maris, X. Wang, M. Simard, J. D. Wuest, *J. Am. Chem. Soc.* **2005**, *127*, 10008–10009.

[8] a) J. D. Dunitz, *Chem. Commun.* **2003**, 545–548; b) G. R. Desiraju, *Nat. Mater.* **2002**, *1*, 77–79; c) A. Gavezzotti, *Acc. Chem. Res.* **1994**, *27*, 309–314; d) J. Maddox, *Nature* **1988**, *335*, 201.

[9] a) *Magnetic Properties of Organic Materials* (Ed.: P. Lahti), Marcel Dekker, New York, **1999**; b) *Magnetism, Vols. 1–3: Molecules to Materials* (Eds.: J. Miller, M. Drillon), Wiley-VCH, Weinheim, **2001**.

[10] R. G. Hicks, M. T. Lemaire, L. Öhrström, J. F. Richardson, L. K. Thompson, Z. Xu, *J. Am. Chem. Soc.* **2001**, *123*, 7154–7159.

[11] A. Alberola, R. J. Less, C. Pask, J. M. Rawson, F. Palacio, P. Oliete, C. Paulsen, A. Yamaguchi, R. D. Farley, D. M. Murphy, *Angew. Chem.* **2003**, *113*, 4930–4933; *Angew. Chem. Int. Ed.* **2003**, *42*, 4782–4785.

[12] a) E. Hernandez, M. Mas, E. Molins, C. Rovira, J. Veciana, *Angew. Chem.* **1993**, *105*, 919–921; *Angew. Chem. Int. Ed. Engl.* **1993**, *32*, 882–884; b) J. Cirujeda, L. Ochando, J. Amigo, C. Rovira, J. Veciana, *Angew. Chem.* **1995**, *107*, 99–102; *Angew. Chem. Int. Ed. Engl.* **1995**, *34*, 55–57; c) J. Cirujeda, M. Mas, E. Molins, F. Lanfranc de Panthou, J. Laugier, J. Park, C. Paulsen, P. Rey, C. Rovira, J. Veci-

ana, *J. Chem. Soc. Chem. Commun.* **1995**, 709–710; d) J. Cirujeda, E. Hernandez-Gasio, C. Rovira, J.-L. Stranger, P. Turek, J. Veciana, *J. Mater. Chem.* **1995**, *5*, 243–252; e) J. Veciana, J. Cirujeda, C. Rovira, E. Molins, J. Novoa, *J. Phys. I* **1996**, 1967–1986; f) T. Sugawara, M. Matsushita, A. Isuoka, N. Wada, N. Takeda, M. Ishikawa, *J. Am. Chem. Soc.* **1997**, *119*, 4369–4379.

[13] T. Akita, K. Kobayashi, *Adv. Mater.* **1997**, *9*, 346–349.

[14] a) N. Yoshioka, M. Irisawa, Y. Mochizuki, K. Tano, H. Inoue, S. Ohba, *Chem. Lett.* **1997**, *26*, 251–252; b) N. Yoshioka, M. Irisawa, Y. Mochizuki, T. Aoki, H. Inoue, *Mol. Cryst. Liq. Cryst. Sci. Technol. Sect. A* **1997**, *306*, 403–408.

[15] J. Ferrer, P. D. Lahti, C. George, G. Antonerra, F. Palacio, *Chem. Mater.* **1999**, *11*, 2205–2210.

[16] A. Lang, Y. Pei, L. Ouahab, O. Khan, *Adv. Mater.* **1996**, *8*, 60–62.

[17] R. Feher, D. Amabilino, K. Wurst, J. Veciana, *Mol. Cryst. Liq. Cryst. Sci. Technol. Sect. A* **1999**, *334*, 333–345.

[18] L. Catala, R. Feher, D. Amabilino, K. Wurst, J. Veciana, *Polyhedron* **2001**, *20*, 1563–1569.

[19] a) F. Romero, R. A. Ziessel, A. De Cian, J. Fischer, P. Turek, *New J. Chem.* **1996**, *20*, 919–924; b) F. Romero, R. Ziessel, M. Drillon, J.-L. Tholence, C. Paulsen, N. Kyritsakas, J. Fischer, *Adv. Mater.* **1996**, *8*, 826–829; c) F. Romero, R. Ziessel, M. Bonnet, Y. Potillon, E. Ressouche, J. Schweitzer, B. Delley, A. Grand, C. Paulsen, *J. Am. Chem. Soc.* **2000**, *122*, 1298–1309.

[20] a) K. Inoue, H. Iwamura, *Chem. Phys. Lett.* **1993**, *207*, 551–554; b) O. Félix, M. W. Hosseini, A. De Cian, J. Fischer, L. Catala, P. Turek, *Tetrahedron Lett.* **1999**, *40*, 2943–2946; c) C. Stroh, F. Romero, N. Kyritsakas, L. Catala, P. Turek, R. Ziessel, *J. Mater. Chem.* **1999**, *9*, 875–882; d) D. Maspoch, L. Catala, P. Gerbier, D. Ruiz-Molina, J. Vidal-Gancedo, K. Wurst, C. Rovira, J. Veciana, *Chem. Eur. J.* **2002**, *8*, 3635–3645; e) M. Minguet, D. Amabilino, J. Cirujeda, K. Wurst, I. Mata, E. Molins, J. Novoa, J. Veciana, *Chem. Eur. J.* **2000**, *6*, 2350–3361; f) M. Baskett, P. D. Lahti, *Polyhedron* **2005**, *24*, 2645–2652.

[21] T. Otsuka, T. Okuno, K. Awaga, T. Inabe, *J. Mater. Chem.* **1998**, *8*, 1157–1163.

[22] M. Ballester, *Acc. Chem. Res.* **1985**, *18*, 380–387.

[23] K. Kobayashi, T. Shirasaka, A. Sato, E. Horn, N. Furukawa, *Angew. Chem.* **1999**, *111*, 3692–3694; *Angew. Chem. Int. Ed.* **1999**, *38*, 3483–3486.

[24] a) G. R. Desiraju, *Crystal Engineering: The Crystal as a Supramolecular Entity, Vol. 2: Perspectives in Supramolecular Chemistry*, Wiley, New York, **1996**; b) J. Bernstein, M. Etter, L. Leiserowitz, *Structure Correlation, Vol. 2*, Wiley, New York, **1994**, Chapter 11.

[25] D. Maspoch, N. Domingo, D. Ruiz-Molina, K. Wurst, J. Tejada, C. Rovira, J. Veciana, *J. Am. Chem. Soc.* **2004**, *126*, 730–731.

[26] D. Maspoch, N. Domingo, D. Ruiz-Molina, K. Wurst, G. Vaughan, J. Tejada, C. Rovira, J. Veciana, *Angew. Chem.* **2004**, *116*, 1864–1868; *Angew. Chem. Int. Ed.* **2004**, *43*, 1828–1832.

[27] Only a few examples of hexa-acid molecules have been reported in the literature. See: a) S. Darlow, *Acta Crystallogr.* **1961**, *14*, 159–166; b) J. Podlaha, I. Cisarova, P. Holy, J. Zavada, *Z. Kristallogr. New Cryst. Struct.* **1999**, *214*, 185–186; c) J. Beeson, L. Fitzgerald, J. Gallucci, R. Gerkin, J. Rademacher, A. Czarnick, *J. Am. Chem. Soc.* **1994**, *116*, 4621–4622.

[28] To the best of our knowledge, only one example of an octa-acid has been reported. See: P. Holy, P. Sehnal, M. Tichy, J. Zavada, I. Cisarova, *Tetrahedron: Asymmetry* **2004**, *15*, 3805–3810.

[29] B. Venkataramanan, W. L. G. James, J. J. Vittal, V. Suresh, *Cryst. Growth Des.* **2004**, *4*, 553–561.

[30] A preliminary communication of this work has already been published. See: N. Roques, D. Maspoch, N. Domingo, K. Wurst, J. Tejada, C. Rovira, J. Veciana, *Chem. Commun.* **2005**, 4801–4803.

[31] a) M. Ballester, J. Riera, J. Castañer, C. Rovira, O. Armet, *Synthesis* **1986**, 64–66; b) D. Ruiz-Molina, J. Veciana, F. Palacio, C. Rovira, *J. Org. Chem.*, **1997**, *62*, 9009–9017.

[32] Diazomethane was prepared from Diazald (Aldrich) by a well-documented procedure. See: Technical Bulletin AL113, Aldrich, Milwaukee, WI, **2000**.

[33] Radicals **1** and **6** have very similar UV/Visible spectra, with absorption bands characteristic of PTM radicals at 380 and 550 nm. See: M. Ballester, J. Riera, J. Castañer, A. Rodríguez, C. Rovira, J. Veciana, *J. Org. Chem.* **1982**, *47*, 4498–4505.

[34] O. Armet, J. Veciana, C. Rovira, J. Riera, J. Castaner, E. Molins, J. Rius, C. Miratvilles, S. Olivilla, J. Brichfeus, *J. Phys. Chem.* **1987**, *91*, 5608.

[35] a) S. Dale, M. Elsegood, A. Coombs, *Cryst. Eng. Comm.*, **2004**, *6*, 328; b) S. Dale, M. Elsegood, *Acta Crystallogr. Sect. E* **2003**, *59*, o1205.

[36] T. Steiner, *Angew. Chem.* **2002**, *114*, 50–80; *Angew. Chem. Int. Ed.* **2002**, *41*, 48.

[37] Poor quality crystals were always obtained on diffusion of *n*-hexane into THF or Et_2O solutions of **6**.

[38] Determined by using A. M. C. T. PLATON, Utrecht University, Utrecht, The Netherlands, A. L. Spek, **1998**.

[39] M. Ballester, J. Riera, J. Castañer, C. Badia, J. Monso, *J. Am. Chem. Soc.* **1971**, *93*, 2215–2225.

[40] Similar oxidations have been reported to occur slowly on treatment of PTMMC and PTMMI (PTM substituted with an iodine atom in the *para* position) with concentrated nitric acid at room temperature. See: M. Ballester, J. Riera, J. Castañer, A. Ibañez, J. Pujadas, *J. Org. Chem.* **1982**, *47*, 259–264.

[41] Such dihedral angles and the bond lengths exhibited by **10** are in agreement with those previously reported for the fully chlorinated fuchsone. See: E. Molins, J. Rius, C. Miratvilles, *Z. Kristallogr. New Cryst. Struct.* **1984**, *169*, 149–158.

[42] The dihedral angles in the motif (O7-C14-C3-O5 = 54°), together with bond lengths and IR data, enable us to discount the formation of any cyclic hydrogen bonding involving the ketone function similar to that encountered in some β-diketone derivatives. See: G. Gilli, F. Bellucci, F. Feretti, G. Gilli, *J. Am. Chem. Soc.* **1989**, *111*, 1023–1028.

[43] Similar bond lengths and dihedral angles have been encountered in the case of cubanecarboxylic acid derivatives presenting the *syn,anti*-catemer motive. See: S. Kuduva, D. Craig, A. Nangia, G. R. Desiraju, *J. Am. Chem. Soc.* **1999**, *121*, 1936–1944.

[44] To the best of our knowledge, *syn,anti*-catemer motifs have been only reported in reference [43], in phenylpropiolic acid derivatives and in monocarboxylic acid derivatives RCOOH with small R substituents, α-oxalic, formic, acetic, and β-terolic acids. See: a) G. R. Desiraju, B. Murty, K. Kishan, *Chem. Mater.* **1990**, *2*, 447–449; b) D. Das, R. Jetti, R. Boese, G. R. Desiraju, *Cryst. Growth Des.* **2003**, *3*, 675–681; c) D. Das, G. R. Desiraju, R. Jetti, R. Boese, *Acta Crystallogr. Sect. E* **2005**, *61*, O1588–O1589; d) J. Derissen, P. Smit, *Acta Crystallogr. Sect. B* **1974**, *30*, 2240–2242; e) I. Nahringbauer, *Acta Crystallogr. Sect. B* **1978**, *34*, 315–318; f) V. Benghiat, L. Leisserowitz, *J. Chem. Soc. Perkin Trans. 2* **1972**, 1763–1972.

[45] a) D. Maspoch, D. Ruiz-Molina, K. Wurst, N. Domingo, M. Cavallini, F. Biscarini, J. Tejada, C. Rovira, J. Veciana, *Nat. Mater.* **2003**, *2*, 190–195; b) D. Maspoch, D. Ruiz-Molina, K. Wurst, C. Rovira, J. Veciana, *Chem. Commun.* **2004**, 1164–1165; c) D. Maspoch, N. Domingo, D. Ruiz-Molina, K. Wurst, J.-M. Hernández, G. Vaughan, C. Rovira, F. Lloret, J. Tejada, J. Veciana, *Chem. Commun.* **2005**, 5035–5037.

Received: March 31, 2006
Published online: September 12, 2006

